

**Simulation and theoretical analysis for stochastic  
dynamics of biochemical networks**

**(生化学ネットワークの確率論的ダイナミクスのシ  
ミュレーションと理論解析)**

**A.B.M. Shamim Ul Hasan**

# Table of Contents

	Page
Table of Contents.....	ii
List of Publications.....	vi
Abstract.....	vii
Acronyms .....	ix
List of Figures.....	x
List of Tables.....	xii
<b>Chapter 1: Introduction .....</b>	<b>1</b>
1.1 Background and motivation .....	1
1.2 System biology and synthesis biology.....	1
1.3 Gene expression .....	2
1.3.1 Transcription.....	2
1.3.2 Translation.....	3
1.3.3 Gene expression by activator and repressor.....	4
1.4 Necessity to study gene regulatory network.....	5
1.5 Noise in gene expression.....	6
<b>Chapter 2: Simplification of gene expression model.....</b>	<b>7</b>
2.1 Introduction.....	7
2.2 Modelling of gene expression .....	8
2.3 Deterministic modelling .....	8
2.4 Stochastic modeling .....	9
2.5 Deterministic vs stochastic simulations .....	10
2.5.1 Simple gene regulation network .....	10

2.6	Conclusion.....	13
Chapter 3:	<b>Noise analysis among different cascades of gene regulatory networks.....</b>	<b>14</b>
3.1	Introduction.....	14
3.2	Methods and Materials .....	14
3.2.1	Open-loop system ACN and RCN model.....	14
3.2.2	Closed-loop system ACN and RCN model .....	17
3.3	Results and discussion .....	20
3.3.1	Noise analysis of open-loop system ACN and RCN model.....	21
3.3.2	Noise analysis of closed-loop system ACN and RCN model.....	25
3.4	Conclusion.....	30
Chapter 4:	<b>Gene expression noise can induce stochastic bimodality, even multimodality in deterministically monostable description with non-cooperative binding.....</b>	<b>31</b>
4.1	Introduction.....	31
4.2	Methods and Materials .....	32
4.2.1	The regulated tMAN model .....	32
4.2.2	The regulated tMRN model.....	34
4.3	Results and discussion.....	35
4.3.1	Robustness of bimodal, multimodal in the tMAN.....	35
4.3.2	Robustness of bimodal, multimodal in the tMRN.....	37
4.4	Discussion.....	39
4.5	Conclusions.....	39
Chapter 5:	<b>Mathematical comparison of memory functions between mutual activation and repression networks in a stochastic environment.....</b>	<b>41</b>

5.1	Introduction.....	41
5.2	Methods.....	44
5.2.1	Competitive network models .....	44
5.2.2	Mathematical comparison.....	47
5.2.3	Time-course simulation of memory.....	49
5.2.4	Potential and probability density.....	50
5.2.5	Mean first-passage time analysis.....	52
5.2.6	Theoretical comparison between the MAN and MRN models....	54
5.2.7	Calculation.....	54
5.3	Results.....	55
5.3.1	MAN-enhanced memory function.....	55
5.3.2	MRN-generated memory function.....	57
5.3.3	Simulation comparison between the MAN and MRN models...	59
5.3.4	Comparison of the stochastic potential profile between the MAN and MRN models.....	62
5.3.5	Comparison of the MFPT between the MAN and MRN models	64
5.4	Discussion .....	<b>69</b>
Chapter 6:	<b>Conclusion and Future Works.....</b>	<b>74</b>
6.1	Conclusion .....	74
6.2	Extended to future works.....	75
Appendix A	.....	77
Appendix B	.....	78
Appendix C	.....	80
Appendix D	.....	82
Appendix E	.....	84

Appendix F .....	86
References .....	88
Acknowledgement .....	95

## List of Publication

1. **A.B.M. Shamim Ul Hasan**, Hiroyuki Kurata: Mathematical comparison of memory functions between mutual activation and repression networks in a stochastic environment. *Journal of Theoretical Biology (accepted)*, 2017.
2. **A.B.M. Shamim Ul Hasan**, Hiroyuki Kurata: Competitive Memory Functions in Gene Regulatory Network. *Information Processing Society 47th Bio and Information Science Society of guidance ( IPSJ)*, Vol. 2, pp. 1-3. 2016-BIO-47
3. **A.B.M. Shamim Ul Hasan**, Hiroyuki Kurata: Gene expression noise can induce stochastic bimodality, even multimodality in deterministically monostable description with non-cooperative binding. *Bioinformatics and Biostatistics for Agriculture, health and Environment*, 2017, ISBN: 978-984-34-0996-6, pp. 397-405.
4. **A.B.M. Shamim Ul Hasan**, Hiroyuki Kurata: Robustness of Memory Functions between Competitive Genes Regulatory Network. *Proceedings of 4th International Symposium on Applied Engineering and Sciences (SAES2016)*, Kitakyushu-shi, **Japan**, Paper-B17, Dec 17-18, 2016.

## Abstract

Stochasticity in gene regulatory network has become increasingly distinguished in the current thinking of system biology. So it is important to know the variety of noise in gene regulatory network. Here, we constructed different types of gene regulatory networks, two-gene regulated mutual activation network of positive feedback; two-gene regulated mutual repression network of positive feedback. We have investigated the dynamical behavior of noise i.e. noise induced bistable (bimodal), multistable (multimodal) of this gene regulatory networks in deterministic and stochastic approaches at the steady state level. Also, we have investigated the one gene with respect to another one in both deterministic, stochastic environments with non-cooperative transcription factor binding / unbinding on the promoter region by using non-symmetric kinetic parameters to predict the bimodal and multimodal gene expression.

On the other hand, biological memory is a ubiquitous function that can generate a sustained response to a transient inductive stimulus. To better understand this function, we must consider the mechanisms by which different structures of genetic networks achieve memory. Here, we investigated two competitive gene regulatory network models: the regulated mutual activation network (MAN) and the regulated mutual repression network (MRN). Stochasticity deteriorated the memory function of both the MAN and the MRN models.

Theoretical analysis was performed to support the simulation results. We exemplified the stochastic potential profile of the one-variable rate equation deriving from the MAN and MRN models. In the presence of noise, a stochastic potential and the mean first-time passage (MFTP) are used to investigate bistability and memory persistency by the Fokker-Planck equation (FPE), which is derived from the chemical Langevin equation.

Mathematical comparison by simulation and theoretical analysis identified functional differences in the stochastic memory between the competitive models: specifically, the MAN provided much more robust, persistent memory than the MRN. The stochastic memory pattern of the MAN can be adjusted by changing the binding strength of the activators, whereas the MRN required highly cooperative and strong binding repressors for robust memory.

Therefore, we should select the MAN or MRN for an optimal, rational design. If a robust memory is required, a mutual activation network should be selected. If the opposite state of protein synthesis is necessary, a mutual repression network must be selected, although the memory effect is fragile. This fragility may be related to the fact that suppression cascades amplify noise compared with activation cascades. A mutual activation network comprising two protein kinases, p42 MAPK and Cdc2, is suggested to require robust memory. On the other hand, a mutual repression network comprising the cI and Cro proteins would require a gene expression system opposite to that of robust memory. A Notch-Delta mutual repression network is an intelligible example to communicate between neighboring cells. An increase in Notch activity within a cell decreases Notch activity in neighboring cells, and thus Notch-Delta mutual repression provides inhomogeneous or opposite protein synthesis in homogeneous cell populations. Our results expected to have significant implications on the dynamical behavior of the genetic network in cell populations.

## Acronyms

ACN :Regulated activator cascade network

RCN :Regulated repressor cascade network

MAN :Regulated mutual activation network

MRN :Regulated mutual repression network

MFPT :Mean First Passage Time

## List of Figures

Figure		Page
1.1	The Schematic models of the gene expression .....	3
1.2	The Schematic models of gene expression by activator and repressor...	4
2.1	The network map of the simple gene regulation .....	11
2.2	Deterministic and stochastic simulations of the simple gene regulation network. ....	12
3.1	The network map of the open-loop system ACN model.....	15
3.2	The network map of the open-loop system RCN model.....	17
3.3	The network map of the closed-loop system ACN model.....	18
3.4	The network map of the closed-loop system RCN model.....	20
3.5	Stochastic simulations of open-loop system ACN and RCN model for strong dissociation constant .....	22
3.6	Stochastic simulations of open-loop system ACN and RCN model for weak dissociation constant .....	23
3.7	Comparisons of open-loop system between ACN and RCN model....	24
3.8	Stochastic simulations of closed-loop system ACN and RCN model for strong dissociation constant.....	27
3.9	Stochastic simulations of closed-loop system ACN and RCN model for weak dissociation constant.....	28
3.10	Comparisons of the closed-loop system between ACN and RCN model...	29
4.1	The network map of the tMAN model.....	33
4.2	The network map of the tMRN model.....	34

4.3	Deterministic and stochastic simulations of the tMAN model for non-cooperative binding.....	36
4.4	Deterministic and stochastic simulations of the tMRN model for non-cooperative binding.....	38
5.1	Two competitive network maps.....	46
5.2	Deterministic and stochastic simulations of the MAN.....	56
5.3	Deterministic and stochastic simulations of the MRN.....	58
5.4	Comparisons of the memory regions among the two competitive models..	61
5.5	Comparisons of the stochastic bistable regions between the two competitive models.....	63
5.6	Comparisons of the MFPTs between the two competitive models.....	66
5.7	Comparison of the probability density of the steady-state level between the two competitive models.....	68
6.1	MRN-NA. Negative autoregulations are added to the MRN model.....	75
6.2	Two competitive oscillator network maps.....	76
E1	Probability density of the MAN and MRN models.....	84
F1	Stochastic potential profile of the MAN and MRN models.....	86

## List of Tables

Table		Page
3.1	List of kinetic parameters used in the open-loop ACN and RCN model .....	16
3.2	List of kinetic parameters used in the closed loop ACN and RCN model.....	19
4.1	List of kinetic parameters used in the tMAN and tMRN models.....	33
5.1	List of kinetic parameters used in gene regulatory networks .....	47
5.2	Steady-state levels of gene expression in the MAN and MRN models.....	48
5.3	Corresponding kinetic parameters for the two competitive models.....	49

# CHAPTER1

## Introduction

### 1.1 Background and motivation

### 1.2 System biology and synthetic biology

The study of the mechanisms underlying complex biological processes as integrated systems of many interacting components of living cells has led to the development of two new fields: systems biology (Ideker T et al., 2001, Adam P, 2001, Kitano, H 2002, Csete, M. E. et al. 2002, Doyle F.J.et al., 2006) and synthetic biology. Systems biology involves to collection of sets of experimental data into models for the behavior of sets of coupled genes and make proposal of mathematical models that might account for at least some significant aspects of this data set, to understand the behavior of a living organism, from the simplest cell Escherichia coli (E. coli) to more complex living organisms, such as humans. To accurate computer solution of the mathematical equations to obtain numerical predictions, and assessment of the quality of the model by comparing numerical simulations with the experimental data. On the molecular level, the complexity of cellular pathways and networks sometimes makes it difficult to understand or reliably predict the dynamical behavior of a system from knowledge of its components in biochemistry and molecular biology, and therefore there is significant interest in the construction of quantitative and predictive the mathematical models of cellular functions. Thus, systems biology and theoretical biology have revealed the mechanisms of how a biochemical network generates a variety of functions such as switching, amplification, adaptation, pulse generation, oscillation and memory (Kurata et al., 2014).

Synthetic biology is understood as an emerging field which builds on the work in genetics and associated fields over the last few decades (Hasty et al., 2002, Kaern et al., 2003, Pawson and Linding, 2005, Tyo et al., 2007,). It has as one of its aims the expansion of a discipline of biology to design and engineer biologically based parts, novel devices, and systems as well as redesigning existing, natural biological systems and strives to make the engineering of biology easier and more predictable results such as in dynamical behavior in gene regulatory networks. This ability would have thoughtful implications, allowing medical interventions to be carried out at the cellular level.

The above two fields can be shared a focus on quantitative and mathematical modeling of biological processes with the advancement of biotechnologies. Also, this happening together required correspondingly quantitative experimental data sets able to provide an accurate description of these processes as they proceed inside the cell and the proper modeling techniques able to accurately explain and predict the dynamical behavior of biological systems.

### **1.3 Gene expression**

Gene expression is the process by which genetic information are used to synthesize of functional gene products. These products are usually proteins, which go on to perform essential functions as enzymes, hormones, and receptors, for example, genes that code for the amino acid sequences are known as structural genes. The process of gene expression involves two main stages

#### **1.3.1. Transcription**

It is the process of RNA synthesis which controlled by the interaction of promoters and enhancers. Several different types of RNA are produced, including messenger RNA (mRNA),

which specifies the sequence of amino acids in the protein product, plus transfer RNA (tRNA) and ribosomal RNA (rRNA), which play a role in the translation process.

### 1.3.2. Translation

The use of mRNA to direct protein synthesis and the subsequent post-translational processing of the protein molecule. Some genes are responsible for the production of other forms of RNA that play a role in translation thus including transfer RNA (tRNA) and ribosomal RNA (rRNA). In translation, the mature mRNA molecule is used as a template to assemble a series of amino acids to produce a polypeptide with a specific amino acid sequence. The complex in the cytoplasm at which this occurs is called a ribosome. Ribosomes are a mixture of ribosomal proteins and ribosomal RNA (rRNA) and consist of a large subunit and a small subunit.

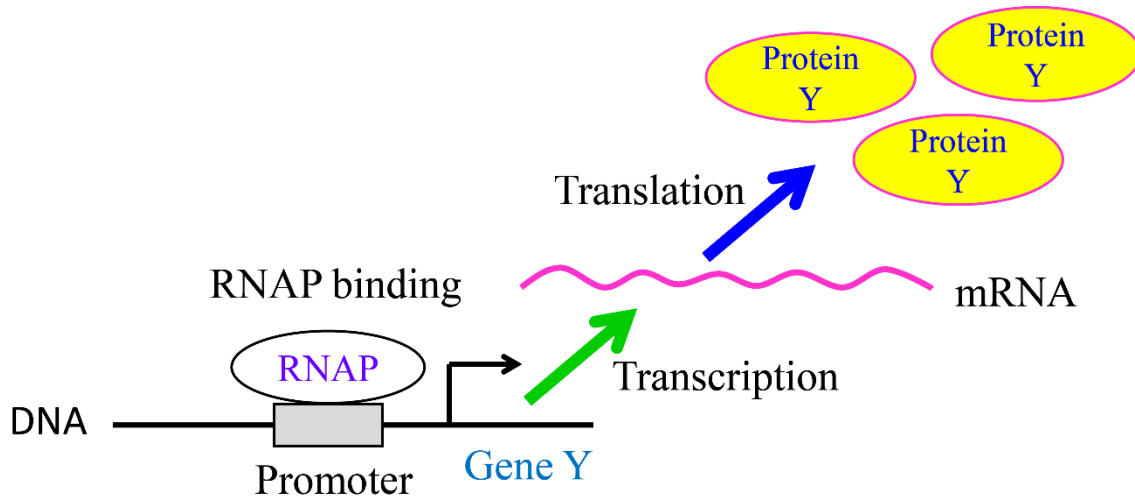


**Fig 1.1. The Schematic models of the gene expression**

Gene regulation may also serve as a substrate for evolutionary change, since control of the timing, location, and amount of gene expression can have a profound effect on the functions (actions) of the gene in a cell or in a multicellular organism.

### 1.3.3 Gene expression by activator and repressor

A transcriptional activator is a protein (transcription factor) that increases gene transcription of a gene or set of genes. Most activators are DNA-binding proteins that bind to enhancers or promoter-proximal elements in which function by binding sequence-specifically to a DNA site located in or near a promoter and making protein-protein interactions with the general transcription machinery (RNA polymerase and general transcription factors), thereby facilitating the binding of the general transcription machinery to the promoter. The DNA site bound by the activator is referred to as an activator site. The part of the activator that makes protein-protein interactions with the general transcription machinery is referred to as an activating region. The part of the general transcription machinery that makes protein-protein interactions with the activator is referred to as an activation target. Therefore, to increase the transcription rate by encouraging the promoter activity.

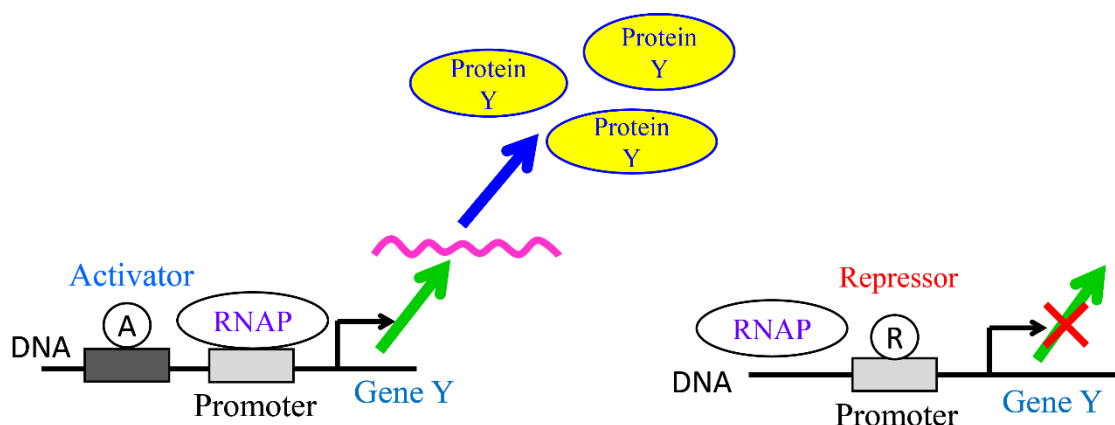


**Fig 1.2. The Schematic models of gene expression by activator and repressor**

In molecular genetics, a repressor is a DNA or RNA binding protein that inhibits the expression of one or more genes by binding to the operator or associated silencers. A DNA-binding repressor blocks the attachment of RNA polymerase to the promoter, thus preventing transcription of the genes into messenger RNA. An RNA-binding repressor binds to the mRNA and prevents translation of the mRNA into protein. This blocking of expression is called repression. Thus, to decrease the transcription rate by inhibiting the binding of RNAP to the promoter.

#### **1.4 Necessity to study gene regulatory network**

Genes are not independent. They regulate each other and act collectively. This collective behavior can be observed using microarray and some genes control the response of the cell to changes in the environment by regulating other genes. Therefore, to study in the genomic area is leading to a complete map of the building blocks of cell biology. This knowledge of this map is in turn to set the stage for a fundamental description of cellular function at the DNA level in the living cell. Moreover, gene regulatory networks have a significant role in every process of life, including cell differentiation, metabolism, the cell cycle and signal transduction also responses to the environment are all controlled by proteins synthesis. Through understanding the dynamics of these gene networks we can shed light on the mechanisms of diseases that occur when these Imperfect cellular developments are dysregulated. Such an explanation will require an understanding of gene regulation, in which proteins often regulate their own production or that of other proteins in a complex web of interactions. This implication of the fundamental logic of genetic networks are sometimes difficult to deduce through experimental techniques alone, and successful approaches will probably involve the union of new experiments and computational modeling techniques (Hasty et.al. 2001.).To use this technique we are able to show the potential discovery of triggering mechanism and treatments for diseases.

## 1.5 Noise in gene expression

Noise in ubiquitous gene regulatory networks are subject to fluctuation disturbances that might occur at various stages such as transcription, translation, transport, chromatin remodeling, and pathway-specific regulation. This noise can come about in two following ways. The noise arises partially from the fluctuations in reaction rates that occur when small numbers of molecules participate in the biochemical processes such as transcription and translation generate "intrinsic" noise. In addition, stochastic fluctuations in the amounts or states of other cellular components lead indirectly to variation in the expression of a particular gene and thus represent "extrinsic" noise that from cell-to-cell differences in the background (Thattai and van Oudenaarden, 2001, Peter S. Swain 2002). Gene expression is a complex and nonlinear system involving numerous components within a cell and always exposed to stochastic fluctuations (McAdams and Arkin, 1997, Zhang et al., 2012). Noise in gene expression is provided by intrinsic fluctuations such as molecular number per cell and uncertainty of kinetic parameters and by extrinsic perturbations deriving from upstream regulators (Blake et al., 2003). The stochastic behaviors of gene expressions and their regulation are essential sources of the observed noise in cellular events (Ozbudak et al., 2002). Translational efficiency is the predominant source of increased noise (Elowitz et al., 2002). While a negative feedback loop suppresses noise, a positive feedback loop can increase the amplitude of noise (Blake et al., 2003), leading to increased cell–cell variability in the target gene output (Eldar and Elowitz, 2010). The miRNA negative feedback loop involving miR-17-92, E2F and Myc in cancer networks reduced noise buffering to improve the signal sensitivity (Zhang et al., 2012).

## CHAPTER 2

### Simplification of gene expression model

#### 2.1 Introduction

Gene expression is a complex that a lot of biochemical processes in the cell involve low number of molecule or infrequent interactions and consequently give rise to stochastic fluctuation (Berg, 1978, McAdams and Arkin, 1997, Ozbudak et al., 2002). The gene expression that occurs in the stochastic diffusion of substances in the cell as well as a regulator by an activator, repressor, negative, positive feedback loop, transcription and translation cascade etc. Noise in gene expression can be characterized by the distribution of protein levels in individual cells and by the timescale of fluctuations, that is, the time over which a cell remains at a given position in the distribution. Modern experimental and hypothetical work has converged on a simple framework to understand gene expression noise. Similar to any physical quantity, gene expression level measurements are subject to noise (Pedraza and van Oudenaarden, 2005). The backgrounds of noise in gene expression proposed a stochastic model for gene expression in eukaryotic (Elowitz et al., 2002, Raser and O'Shea, 2004). Their model suggests that proteins are produced in random bursts in gene expression. As a single mRNA transcript can produce multiple copies of a protein, protein translation amplifies transcriptional noise. Several other models have further legalized and extended this hypothesis by analyzing the mechanisms contributing to noise in gene expression (Eldar and Elowitz, 2010). The numerical simulation of biochemical reactions can be carried out using deterministic or

stochastic approaches. Here we have shown the comparison between two approaches and find out the limitation due to the number of molecules in protein synthesis.

## **2.2 Modelling of gene expression**

The mathematical modeling has been applied to biological systems for decades, but with respect to gene expression, too few molecular components have been known to build useful, predictive models in both experimental and computational methods (Ay and Arnosti, 2011). The modeling of gene regulation is central to such efforts because gene expression is at the nexus of many biological processes that have combined to offer the prospect of developing a quantitative and systematic understanding of system biology, and this has been driven a flow in recent interest in the formulation of mathematical models in biology, especially of the molecular-level details of biochemical kinetics reactions processes (Kurata et al. 2007, Kaerm el al. 2005).

## **2.3 Deterministic modelling**

A deterministic model is developed applying first principals equations that are, mass balance, energy balances, kinetic rates, calculating physio-chemical parameters and so on. It is also called white-box model. These reactions rate of a biochemical reaction are equal to the rate constant multiplied by the product of the concentrations of species that participate in this reaction networks. As a deterministic point of view, with a reaction rate connected with each reaction, the rate of change of the concentration of every species is equal to the rate for this species to be produced minus the rate of this species being consumed or degraded. This concept allows us to consider only the effect of concentration of each species in the system. We have written down the differential equation for the rate of change of concentrations of specie, we can have got a set of coupled or single ordinary differential equations governing the time evolution of the system. Finally, we will be able to get the time evolution of the system of

interest by solving the set of differential equation with certain initial conditions if needed (Eq. 2.1). We have to able to see the set of differential equations with corresponding network reactions. Here, we calculated the ordinary differential equations for deterministic simulation by the MATLAB (Math works).

## **2.4 Stochastic modeling**

A Stochastic model is sometimes called black box modelling. It is known as the input and output values and a non-deterministic model is applied to correlate the variables. The stochastic noise in gene expression which will be usually not negligible (Peter et al. 2006, Thattai and van Oudenaarden, 2001). Because biological systems are successful despite existing in a stochastic environment and despite the probabilistic nature of the biochemical reactions. Expressing biochemical network models by writing out sets of reactions and translating them into deterministic sets of ordinary differential equations does not capture this biological variability, so stochastic modelling approaches are often applied to intracellular biological models (Kaerm el al. 2005). Therefore, by simulating the fluctuations in a small number regimes, such as models can capture the intrinsic noise in biological systems, because the stochasticity arises from fluctuations (noise) in transcription and translation of gene expression is spite of the environmental conditions are constants, but extrinsic noise sources are not obviously handled and must be added by other meanings. Thus, the stochastic model of a biochemical reaction network can be solved by the following the process, it will be either analytically using master equations approach, or numerically using the Gillespie algorithm. It is a discrete and exact procedure in the sense that every reaction in individually simulated. On the other hand, chemical Langevin equation is a continuous process that also represents the molecular evolution. Outstanding to the complexity of master equations and stochastic simulations, approximations to both these two approaches have been described in the chemical

Langevin equation approach. Which gives an approximate solution; for the Tau-leap, Gillespie algorithm, and other similar approaches approximate to the exact Gillespie algorithm (Gillespie, 1977, Cao et al., 2006). Here the Gillespie algorithm was used to perform the stochastic simulation (Kurata et al., 2014)

## **2.5 Deterministic vs stochastic simulations**

Stochastic approaches are different to deterministic simulations (Jose et al. 2003). In the deterministic method, the output of the model is fully determined by the parameter values and the initial conditions. The deterministic models include several classes of models, associate the most usual is represented by systems of ordinary differential equations (Kurata et al. 2014). In here approaches the behavior of the model is predictable. In stochastic models possess some inherent randomness i.e. the probabilistic characteristics are taken into an explanation. Consequently, the entirely predictable character is lost. When large numbers of molecules are present in biochemical reactions usually continue in a predictable manner because the fluctuations are averaged out. However, when only a few molecules take part in a reaction, as typically occurred in a cell, stochastic effects become distinguished. Obviously, the natural world is buffeted by stochasticity. But, stochastic processes are considerably more complicated with compare deterministic approach.

### **2.5.1 Simple gene regulation network**

We constructed the simple model of the gene regulatory network that consists of one gene  $y(1)$  encoding a transcription factor according to the graphical notation (Kurata et al. 2003, Kurata et al. 2007), as shown Fig. 2.1.

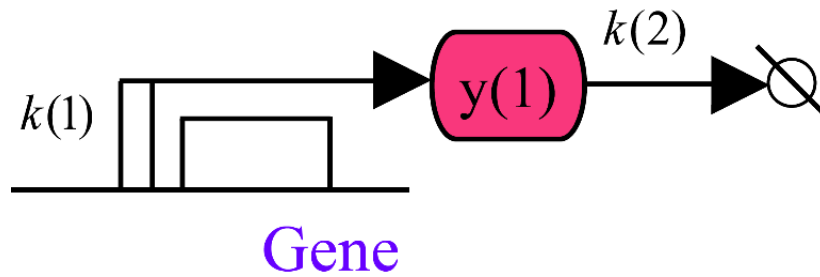


**Fig 2.1. The network map of the simple gene regulation.** Here, the simple regulation protein  $y(1)$  synthesis with the first-order degradation.

The mathematical equation of this model is described by the following:

$$\frac{dy(1)}{dt} = k(1) - k(2) \cdot y(1) \quad (2.1)$$

where  $k(1)$ ,  $k(2)$  are transcription and first-order degradation rate constants respectively.

We have investigated this model for a large number of molecules and a small number of molecules in the comparison between deterministic and stochastic approaches at the steady state level. In both approaches, our simulation results have shown the average behavior is an appropriate representation of the system evolution in protein synthesis when the number of molecules involved is large (Fig. 2.2). In contrast, when the stochastic models can be predicted stochastic effects and give a more accurate representation of the system evolution when this evolution depends on the behavior of a small number of molecules.

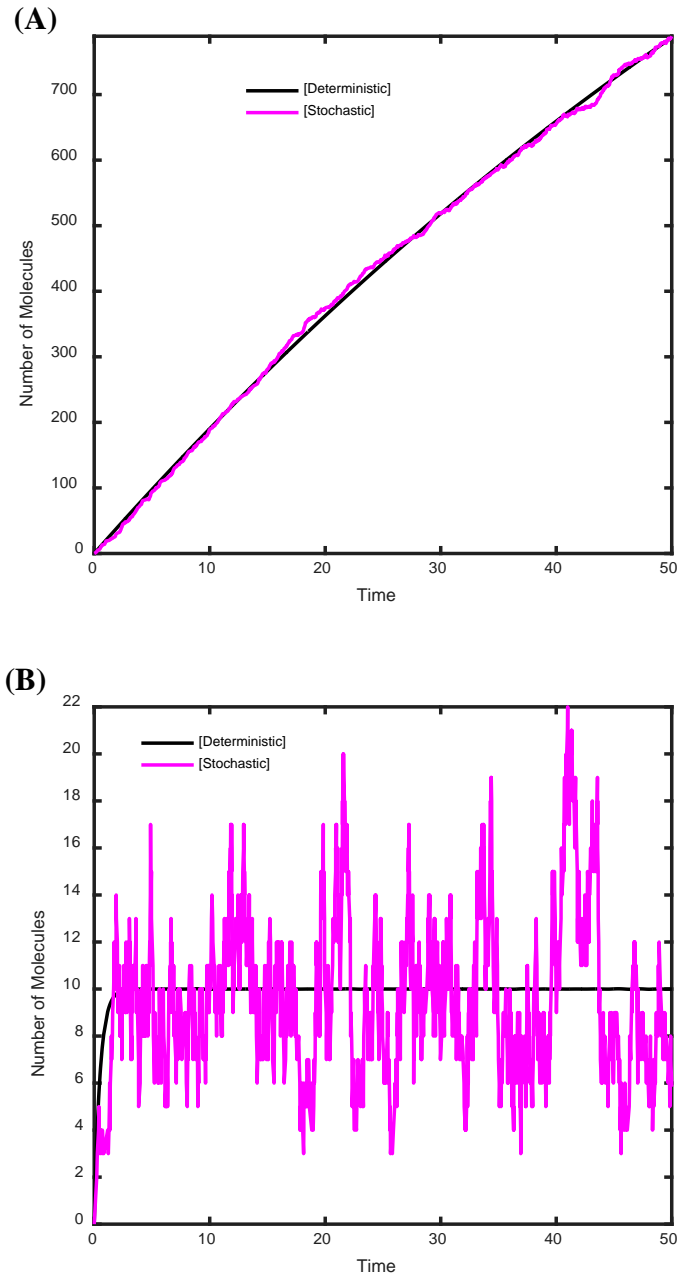


**Fig 2.2. Deterministic and stochastic simulations of the simple gene regulation network.**

(A) Deterministic vs stochastic simulation of protein  $y(1)$  synthesis for a large number of molecules. (B) Deterministic vs stochastic simulation of protein  $y(1)$  synthesis for a small number of molecules.

Thus, the deterministic behavior can be seen as a limitation of the stochastic behavior when the number of molecules is large (Fig. 2.2). Because deterministic simulation is failed to

explain the actual behavior (randomly fluctuating) for the small number of molecules in system biology.

## **2.6. Conclusion**

The Gillespie algorithm provides an exact simulation of the Master equation at a high computational cost, which increases rapidly with the number of species and the system size. It is very attractive for small systems or the small number of molecules to describe fluctuations as well as noise. We observed that the deterministic model is very accurate for large systems with a single study state. But deterministic approximation fails to show large concentration fluctuation for the small number of molecules. Also impossible to predict the motion of (classical) molecules due to the ignorance of positions and velocities of all components of the system (biochemical reactions). Stochastic simulations are best than deterministic when we consider the small number of molecules in system biology.

## **CHAPTER 3**

# **Noise analysis among different cascades of gene regulatory networks**

### **3.1 Introduction**

Gene expression is subject to stochastic fluctuations or noise at the level of their components in cellular functions (Elowitz et al., 2002, Raser and O'Shea, 2004). The genetic networks that regulate the gene expression which can be characteristic by the distribution of protein levels in cellular functions (Eldar and Elowitz, 2010). In this chapter, to solve the distinct feature among the activation, repression or mutual activation-repression-positive feedback, open-loop, the close-loop system of networks under a stochastic environment. We constructed different types of gene regulatory networks, open-loop system activator cascade network (ACN); open-loop system repressor cascade network (RCN); closed-loop system activator cascade network (ACN); closed-loop system repressor cascade network (RCN). We have shown the noise among this gene networks due to mathematical presentations at the steady state level. In general, our results suggested that the strong dissociation constant of repressor cascades always increased the noise of gene expression.

### **3.2 Methods and Materials**

#### **3.2.1 Open-loop system ACN and RCN model**

Here, we constructed the simple models of the gene regulatory networks that consist of four genes encoding a transcription factor according to the graphical notation (Kurata et al.

2003, Kurata et al. 2007), as shown Figs. 3.1, 3.2. The Open-loop system activator cascade network (ACN) consists of  $y(0)$ ,  $y(1)$ ,  $y(2)$  and  $y(3)$  proteins, thus activated with equal strength of dissociation constant rate as shown in Fig.3.1. Here, required outcomes protein synthesis are  $y(1)$ ,  $y(2)$  and  $y(3)$  at the same steady state level. This model is described by the following mathematical equations:

$$\frac{dy(1)}{dt} = k(1) \cdot \frac{y(0)}{K + y(0)} - k(2) \cdot y(1) \quad (3.1)$$

$$\frac{dy(2)}{dt} = k(3) \cdot \frac{y(1)}{K + y(1)} - k(4) \cdot y(2) \quad (3.2)$$

$$\frac{dy(3)}{dt} = k(5) \cdot \frac{y(2)}{K + y(2)} - k(6) \cdot y(3) \quad (3.3)$$

where the employed parameters are described in Table 3.1.

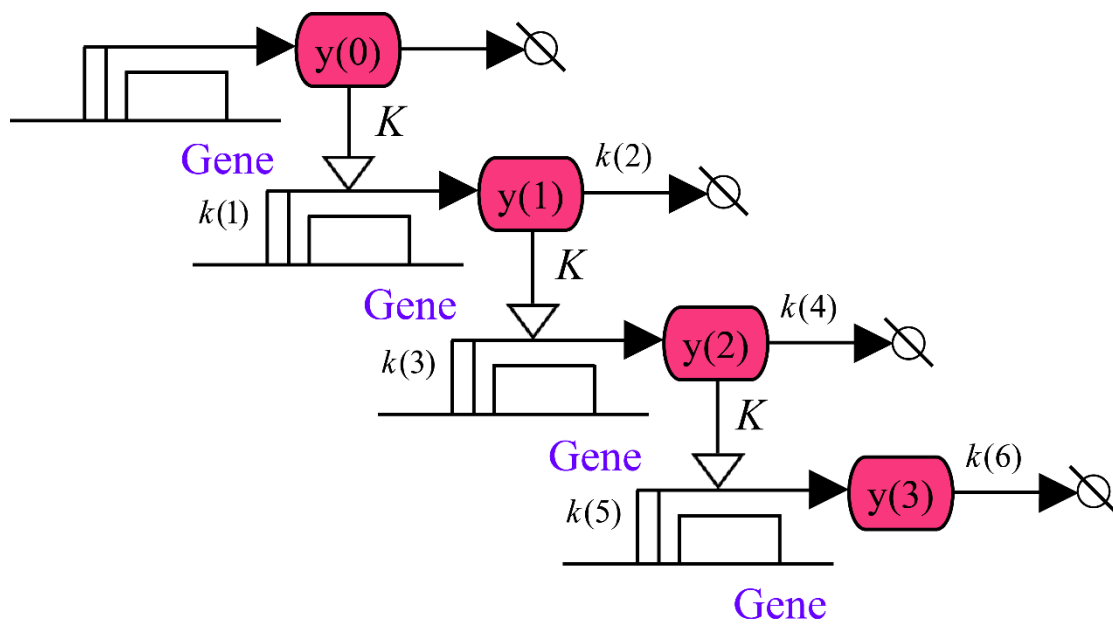


**Fig 3.1. The network map of the open-loop system ACN model.** The activation network cascades consist of  $y(0)$ ,  $y(1)$ ,  $y(2)$  and  $y(3)$  proteins synthesis with the first-order degradation.

**Table 3.1.** List of kinetic parameters used in the open-loop ACN and RCN model

<b>Kinetic parameters</b>	<b>Definition</b>
$k(1), k(3), k(5)$	protein synthesis rate constants
$k(2), k(4), k(6)$	degradation rate constants
$K$	dissociation constant

The open-loop system repressor cascade network (RCN) consists of  $y(0)$ ,  $y(1)$ ,  $y(2)$  and  $y(3)$  proteins, thus repressed with equal strength of dissociation constant rate as shown in Fig. 3.2. Here, required outcomes protein synthesis are  $y(1)$ ,  $y(2)$  and  $y(3)$  at the same steady state level. This model is described by the following mathematical equations:

$$\frac{dy(1)}{dt} = k(1) \cdot \frac{K}{K + y(0)} - k(2) \cdot y(1) \quad (3.4)$$

$$\frac{dy(2)}{dt} = k(3) \cdot \frac{K}{K + y(1)} - k(4) \cdot y(2) \quad (3.5)$$

$$\frac{dy(3)}{dt} = k(5) \cdot \frac{K}{K + y(2)} - k(6) \cdot y(3) \quad (3.6)$$

where the employed parameters are described in Table 3.1.

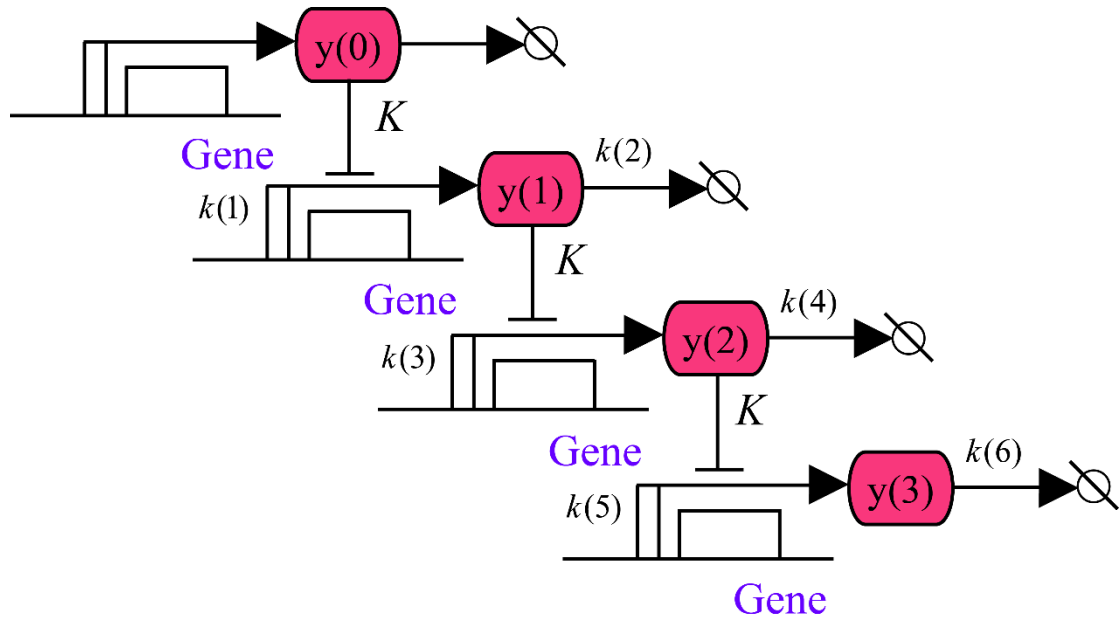


**Fig 3.2. The network map of the open-loop system RCN model.** The repression network cascades consist of  $y(0)$  ,  $y(1)$  ,  $y(2)$  and  $y(3)$  proteins synthesis with the first-order degradation.

### 3.2.2 Closed-loop system ACN and RCN model

Here, we constructed the simple models of the gene regulatory networks that consist of six genes encoding a transcription factor according to the graphical notation (Kurata et al. 2003, Kurata et al. 2007), as shown Figs. 3.3, 3.4. The closed-loop system activator cascade network (ACN) consists of  $y(1)$  ,  $y(2)$  ,  $y(3)$  ,  $y(4)$  ,  $y(5)$  and  $y(6)$  proteins, thus activated with equal strength of dissociation constant rate as shown in Fig.3.3. Here, required outcomes protein synthesis are  $y(1)$  ,  $y(2)$  ,  $y(3)$  ,  $y(4)$  ,  $y(5)$  and  $y(6)$  at the same steady state level. This model is described by the following mathematical equations:

$$\frac{dy(1)}{dt} = k(1) \cdot \frac{y(6)}{K + y(6)} - k(2) \cdot y(1) \quad (3.7)$$

$$\frac{dy(2)}{dt} = k(3) \cdot \frac{y(1)}{K + y(1)} - k(4) \cdot y(2) \quad (3.8)$$

$$\frac{dy(3)}{dt} = k(5) \cdot \frac{y(2)}{K + y(2)} - k(6) \cdot y(3) \quad (3.9)$$

$$\frac{dy(4)}{dt} = k(7) \cdot \frac{y(3)}{K + y(3)} - k(8) \cdot y(4) \quad (3.10)$$

$$\frac{dy(5)}{dt} = k(9) \cdot \frac{y(4)}{K + y(4)} - k(10) \cdot y(5) \quad (3.11)$$

$$\frac{dy(6)}{dt} = k(11) \cdot \frac{y(5)}{K + y(5)} - k(12) \cdot y(6) \quad (3.12)$$

where the employed parameters are described in Table 3.2.

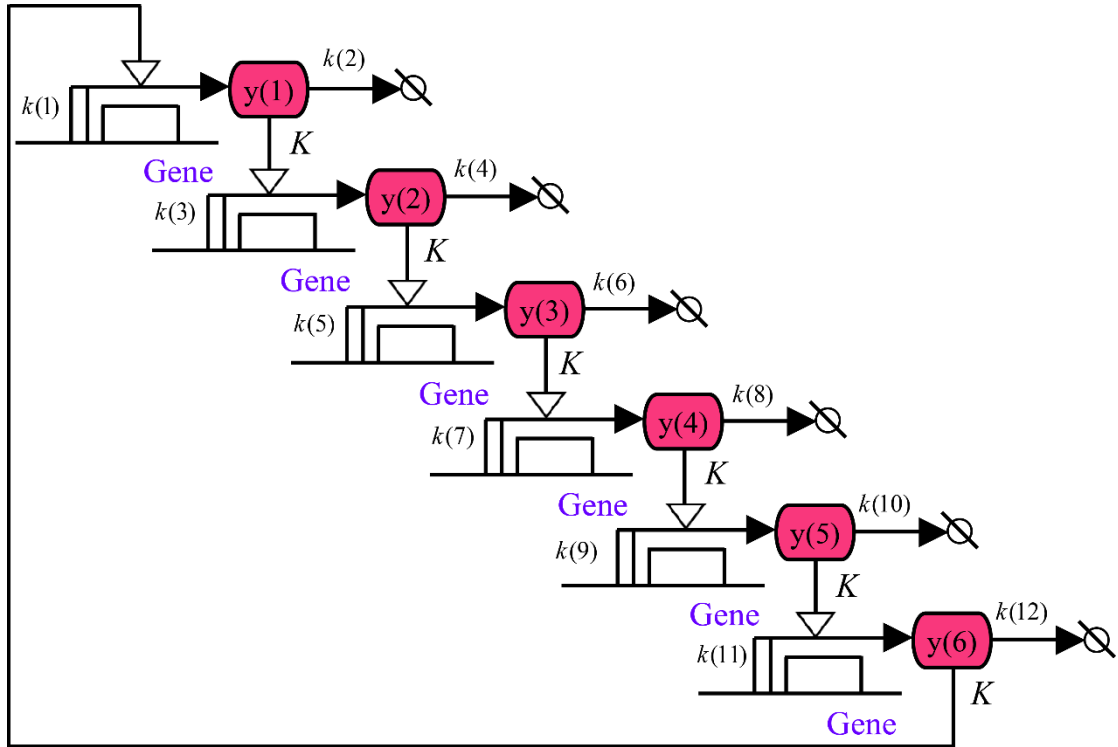


**Fig 3.3. The network map of the closed-loop system ACN model.** The activation network cascades consists of y(1), y(2), y(3), y(4), y(5) and y(6) proteins synthesis with the first-order degradation.

**Table 3.2.** List of kinetic parameters used in the closed loop ACN and RCN model

<b>Kinetic parameters</b>	<b>Definition</b>
$k(1), k(3), k(5), k(7), k(9), k(11)$	protein synthesis rate constants
$k(2), k(4), k(6), k(8), k(10), k(12)$	degradation rate constants
$K$	dissociation constant

The closed-loop system repressor cascade network (RCN) consists of  $y(1)$ ,  $y(2)$ ,  $y(3)$ ,  $y(4)$ ,  $y(5)$  and  $y(6)$  proteins, thus repressed with equal strength of dissociation constant rate as shown in Fig. 3.4. Here, required outcomes protein synthesis are  $y(1)$ ,  $y(2)$ ,  $y(3)$ ,  $y(4)$ ,  $y(5)$  and  $y(6)$  at the same steady state level. This model is described by the following mathematical equations:

$$\frac{dy(1)}{dt} = k(1) \cdot \frac{K}{K + y(6)} - k(2) \cdot y(1) \quad (3.13)$$

$$\frac{dy(2)}{dt} = k(3) \cdot \frac{K}{K + y(1)} - k(4) \cdot y(2) \quad (3.14)$$

$$\frac{dy(3)}{dt} = k(5) \cdot \frac{K}{K + y(2)} - k(6) \cdot y(3) \quad (3.15)$$

$$\frac{dy(4)}{dt} = k(7) \cdot \frac{K}{K + y(3)} - k(8) \cdot y(4) \quad (3.16)$$

$$\frac{dy(5)}{dt} = k(9) \cdot \frac{K}{K + y(4)} - k(10) \cdot y(5) \quad (3.17)$$

$$\frac{dy(6)}{dt} = k(11) \cdot \frac{K}{K + y(5)} - k(12) \cdot y(6) \quad (3.18)$$

where the employed parameters are described in Table 3.2.

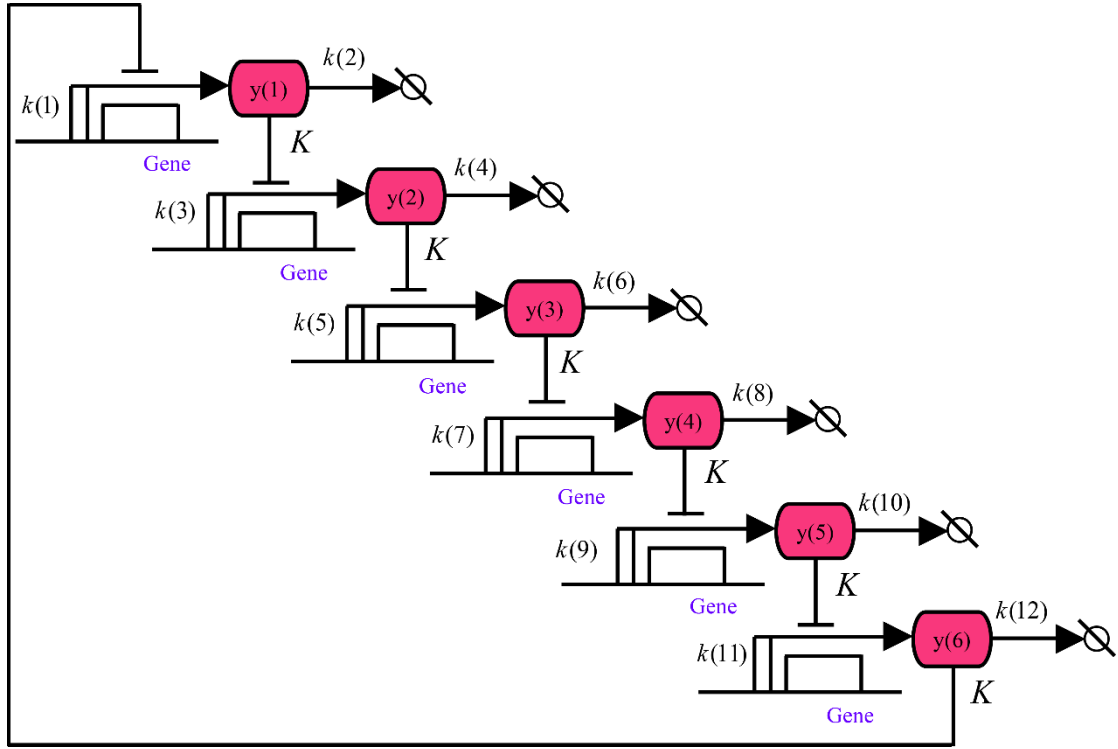


**Fig 3.4. The network map of the closed-loop system RCN model.** The repression network cascades consists of  $y(1)$ ,  $y(2)$ ,  $y(3)$ ,  $y(4)$ ,  $y(5)$  and  $y(6)$  proteins synthesis with the first-order degradation.

The Gillespie algorithm was used to perform the stochastic simulation (Gillespie, 1977). The MATLAB (Mathworks) was employed for this simulation results. We estimated the noise in gene expression by the coefficient of variation (CV) is defined as the ratio of the standard deviation to the mean.

### 3.3 Results and discussion

We have investigated the noise effect just before our proposed of genetic network models at the steady state level when the value of disassociation constant  $K$  is low and high (strong-weak), we compared the stochastic noise while the values of the corresponding kinetic parameters within each model and between the competitive models and the steady state levels.

### 3.3.1 Noise analysis of open-loop system ACN and RCN model

We investigated the open-loop system ACN and RCN model at strong dissociation constants of  $K = 0.01$ , where the other corresponding kinetic parameters were set as synthesis rate  $k(1) = k(3) = k(5) = 10$  and degradation rate  $k(2) = k(4) = k(6) = 1$ . The steady-state simulation of  $y(1)$ ,  $y(2)$  and  $y(3)$  proteins as shown in Fig. 3.5. To estimate the effect of stochasticity, we calculated the CVs of  $y(1)$ ,  $y(2)$  and  $y(3)$  from time 0 to 100, when their steady state levels were the same. The ACN model provided  $CV = 0.303$  for  $y(1)$ ,  $CV = 0.287$  for  $y(2)$  and  $CV = 0.286$  for  $y(3)$ , while RCN model did  $CV = 0.361$  for  $y(1)$ ,  $CV = 0.467$  for  $y(2)$  and  $CV = 0.484$  for  $y(3)$ . The strong binding was suggested to increase the CV in the RCN than ACN model. The increased CV or increased noise among the cascades in both models.

On the other hand, the Fig. 3.6 shown the steady-state stochastic simulation of  $y(1)$ ,  $y(2)$  and  $y(3)$  proteins at weak dissociation constants of  $K = 10$ , where the other corresponding kinetic parameters were set to be the same as previous. To estimate the effect of stochasticity, we calculated the CVs of  $y(1)$ ,  $y(2)$  and  $y(3)$  from time 0 to 100, when their steady state levels were the same. The ACN model provided  $CV = 0.315$  for  $y(1)$ ,  $CV = 0.312$  for  $y(2)$  and  $CV = 0.283$  for  $y(3)$ , while RCN model did  $CV = 0.323$  for  $y(1)$ ,  $CV = 0.385$  for  $y(2)$  and  $CV = 0.473$  for  $y(3)$ . The weak binding was suggested to decrease the CV in the RCN than ACN model. The increased CV or increased noise among the cascades in both models.

To analyze the effect of noise comparisons in ACN and RCN models, we simulated the mean and CV for  $y(1)$ ,  $y(2)$  and  $y(3)$  with respect to a change in dissociation constants of  $K$ , while keeping the same steady-state level (Fig. 3.7). In the ACN model, the CVs of  $y(1)$ ,  $y(2)$  and

$y(3)$  were less than those of the RCN model at a strong dissociation constant, i.e., ACN decreases noise at a strong dissociation constant and vice-versa for weak dissociation constant .

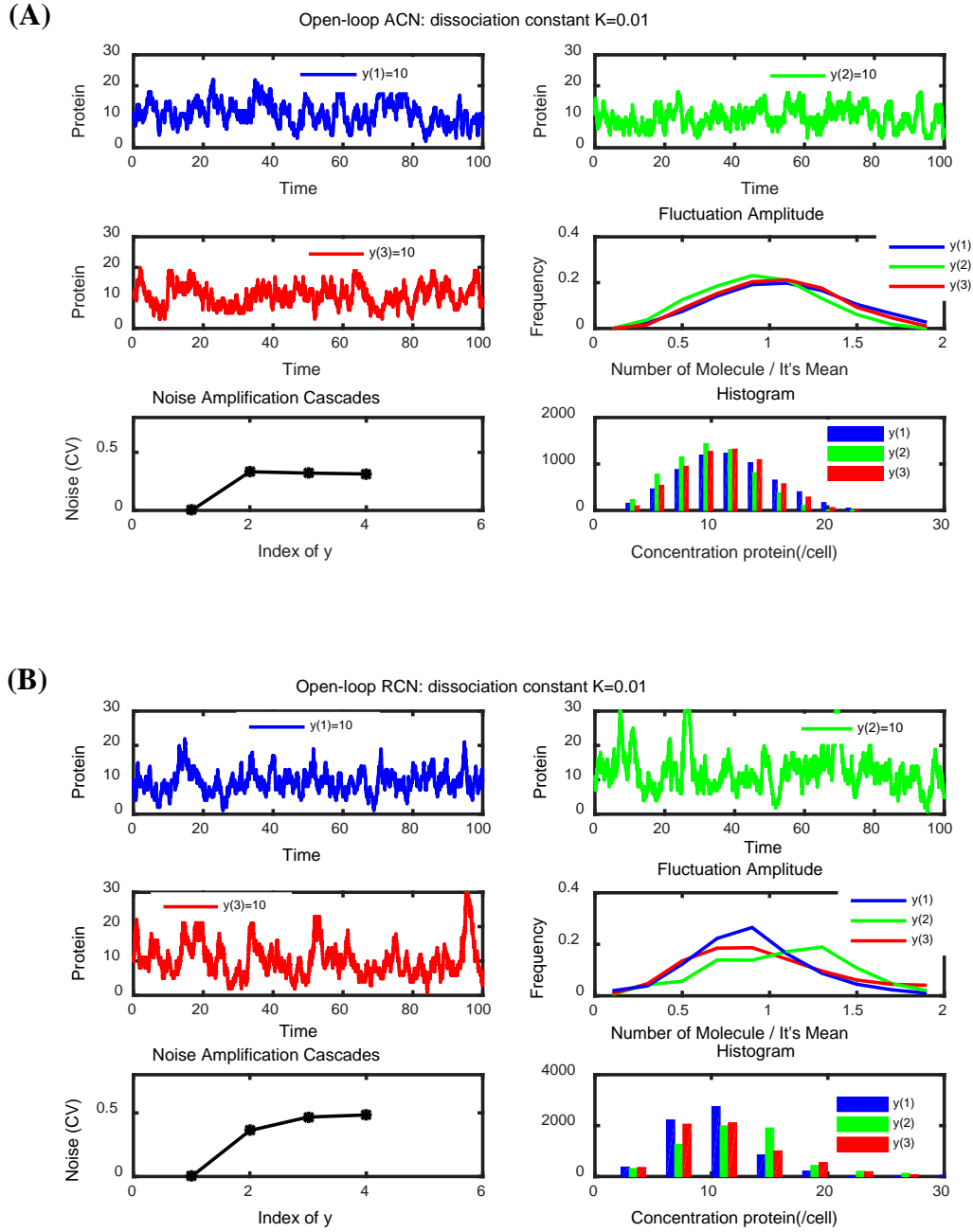


**Fig 3.5. Stochastic simulations of open-loop system ACN and RCN model for strong dissociation constant.** (A) ACN model, (B) RCN model, stochastic simulation of proteins  $y(1)$ ,  $y(2)$  and  $y(3)$  at dissociation constants  $K = 0.01$  with synthesis rate  $k(1) = k(3) = k(5) = 10$  and degradation rate  $k(2) = k(4) = k(6) = 1$ . The blue, green and red appearances indicate  $y(1)$

,  $y(2)$  and  $y(3)$  respectively with the corresponding fluctuations amplitude, noise amplification cascades, and histograms.

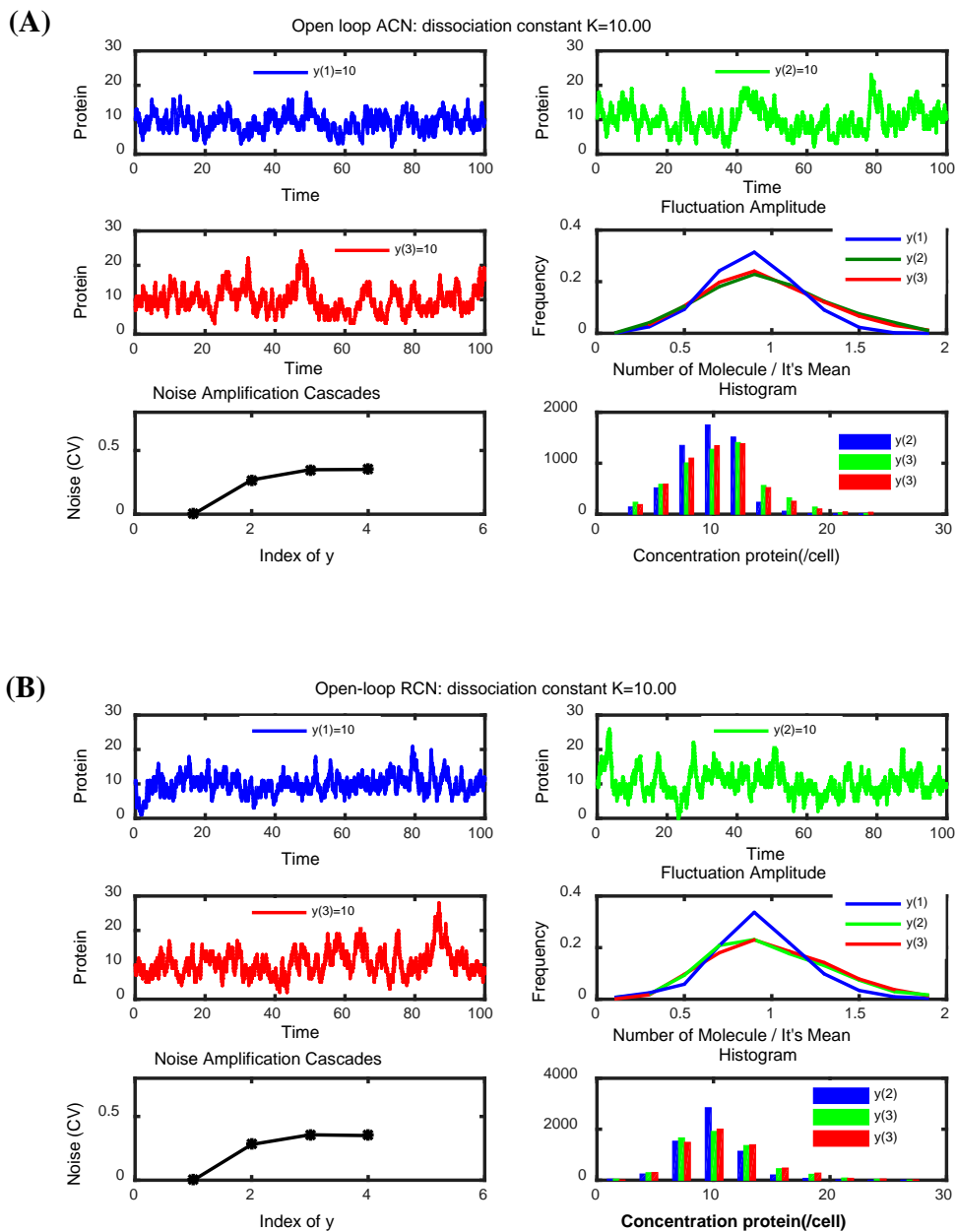


**Fig 3.6. Stochastic simulations of open-loop system ACN and RCN model for weak dissociation constant.**

(A) ACN model, (B) RCN model, stochastic simulation of proteins  $y(1)$ ,  $y(2)$  and  $y(3)$  at dissociation constants  $K = 10$  with synthesis rate  $k(1) = k(3) = k(5) = 10$  and degradation rate

$k(2) = k(4) = k(6) = 1$ . The blue, green and red appearances indicate  $y(1)$ ,  $y(2)$  and  $y(3)$  respectively with the corresponding fluctuations amplitude, noise amplification cascades, and histograms.

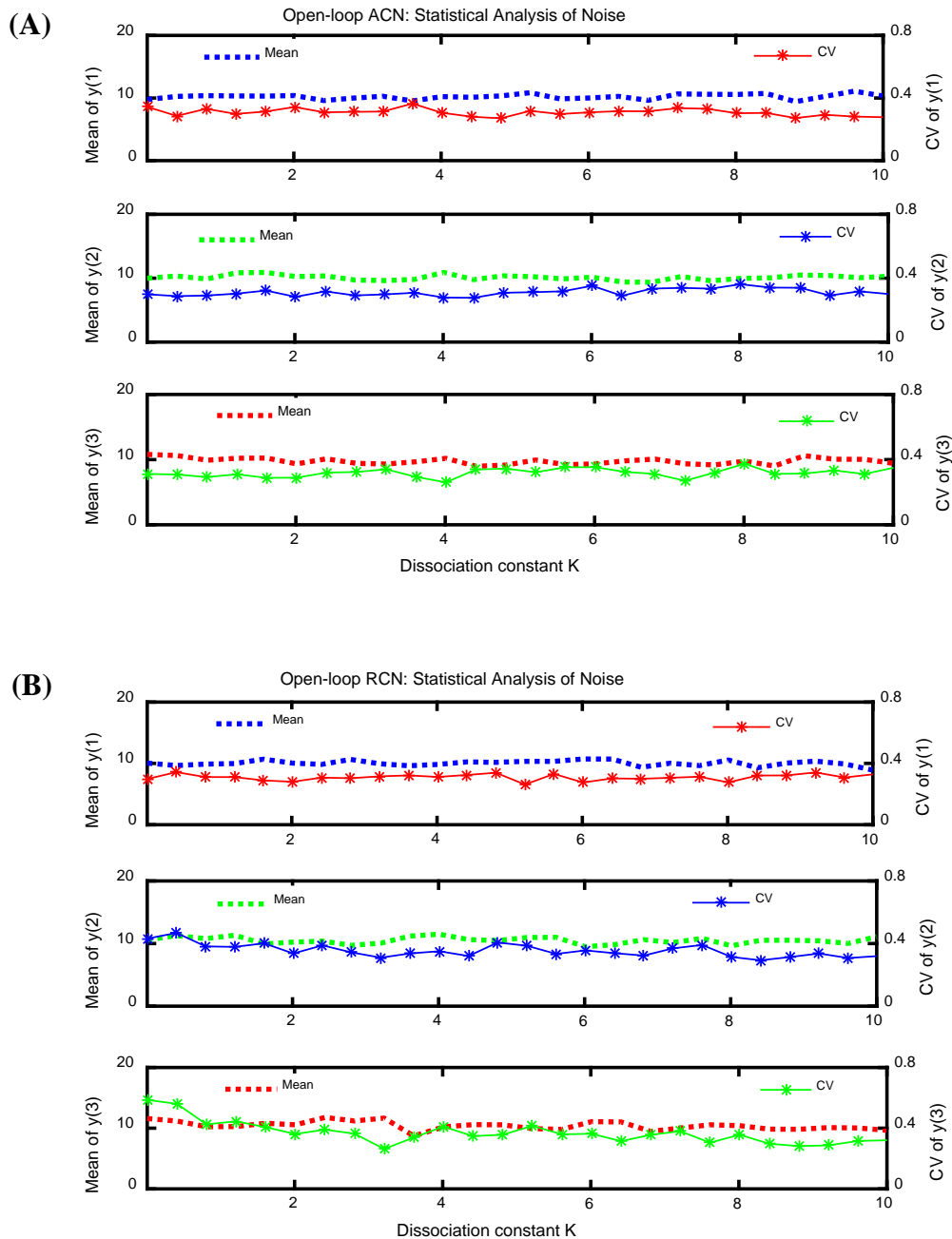


**Fig 3.7. Comparisons of open-loop system between ACN and RCN model**

(A) ACN model, (B) RCN model, stochastic fluctuations between the ACN and RCN models of proteins  $y(1)$ ,  $y(2)$  and  $y(3)$ . The means and CVs are simulated with respect to a change in

dissociation constants  $K$  while keeping the steady state at a constant level among all the models.

### 3.3.2 Noise analysis of closed-loop system ACN and RCN model

We investigated the closed-loop system ACN and RCN model at strong dissociation constants of  $K = 0.1$ , where the other corresponding kinetic parameters were set as synthesis rate  $k(1) = k(3) = k(5) = k(7) = K(9) = k(11) = 10$  and degradation rate  $k(2) = k(4) = k(6) = k(8) = k(10) = k(12) = 1$ . The steady-state simulation of  $y(1)$ ,  $y(2)$ ,  $y(3)$ ,  $y(4)$ ,  $y(5)$  and  $y(6)$  proteins as shown in Fig. 3.8. To estimate the effect of stochasticity, we calculated the CVs of  $y(1)$ ,  $y(2)$ ,  $y(3)$ ,  $y(4)$ ,  $y(5)$  and  $y(6)$  from time 0 to 100, when their steady state levels were the same. The ACN model provided  $CV = 0.328$  for  $y(1)$ ,  $CV = 0.349$  for  $y(2)$ ,  $CV = 0.280$  for  $y(3)$ ,  $CV = 0.313$  for  $y(4)$ ,  $CV = 0.291$  for  $y(5)$  and  $CV = 0.333$  for  $y(6)$ , while RCN model did  $CV = 0.341$  for  $y(1)$ ,  $CV = 6.672$  for  $y(2)$ ,  $CV = 0.310$  for  $y(3)$ ,  $CV = 3.983$  for  $y(4)$ ,  $CV = 0.278$  for  $y(5)$  and  $CV = 3.756$  for  $y(6)$ . The strong binding was suggested to increase the CV in the RCN than ACN model. The increased CV or increased noise among the cascades in both models.

Three cascades  $y(1)$ ,  $y(3)$  and  $y(5)$  are highly stable and others  $y(2)$ ,  $y(4)$  and  $y(6)$  are opposite them when the protein concentration is held at the same level. Because they are affected highly positively and negatively.

Then the Fig. 3.9 shown the steady-state stochastic simulation of  $y(1)$ ,  $y(2)$ ,  $y(3)$ ,  $y(4)$ ,  $y(5)$  and  $y(6)$  proteins at weak dissociation constants of  $K = 50$ , where the other corresponding kinetic parameters were set to be the same as previous.

To estimate the effect of stochasticity, we calculated the CVs of  $y(1)$ ,  $y(2)$ ,  $y(3)$ ,  $y(4)$ ,  $y(5)$  and  $y(6)$  from time 0 to 100, when their steady state levels were the same. The ACN model provided  $CV = 0.461$  for  $y(1)$ ,  $CV = 0.417$  for  $y(2)$ ,  $CV = 0.419$  for  $y(3)$ ,  $CV = 0.417$  for  $y(4)$ ,  $CV = 0.395$  for  $y(5)$  and  $CV = 0.415$  for  $y(6)$ , while RCN model did  $CV = 0.325$  for  $y(1)$ ,  $CV = 0.321$  for  $y(2)$ ,  $CV = 0.364$  for  $y(3)$ ,  $CV = 0.310$  for  $y(4)$ ,  $CV = 0.344$  for  $y(5)$  and  $CV = 0.353$  for  $y(6)$ . The weak binding was suggested to decrease the CV in the RCN than ACN model. The increased CV or increased noise among the cascades in both models.

To evaluate the effect of noise comparisons in ACN and RCN models, we simulated the mean and CV for  $y(1)$ ,  $y(2)$ ,  $y(3)$ ,  $y(4)$ ,  $y(5)$  and  $y(6)$  with respect to a change in dissociation constants of  $K$ , while keeping the same steady-state level (Fig. 3.10). In the ACN model, the CVs of  $y(1)$ ,  $y(2)$ ,  $y(3)$ ,  $y(4)$ ,  $y(5)$  and  $y(6)$  were less than those of the RCN model at strong dissociation constant, i.e., ACN decreases noise at strong dissociation constant and vice-versa for weak dissociation constant .

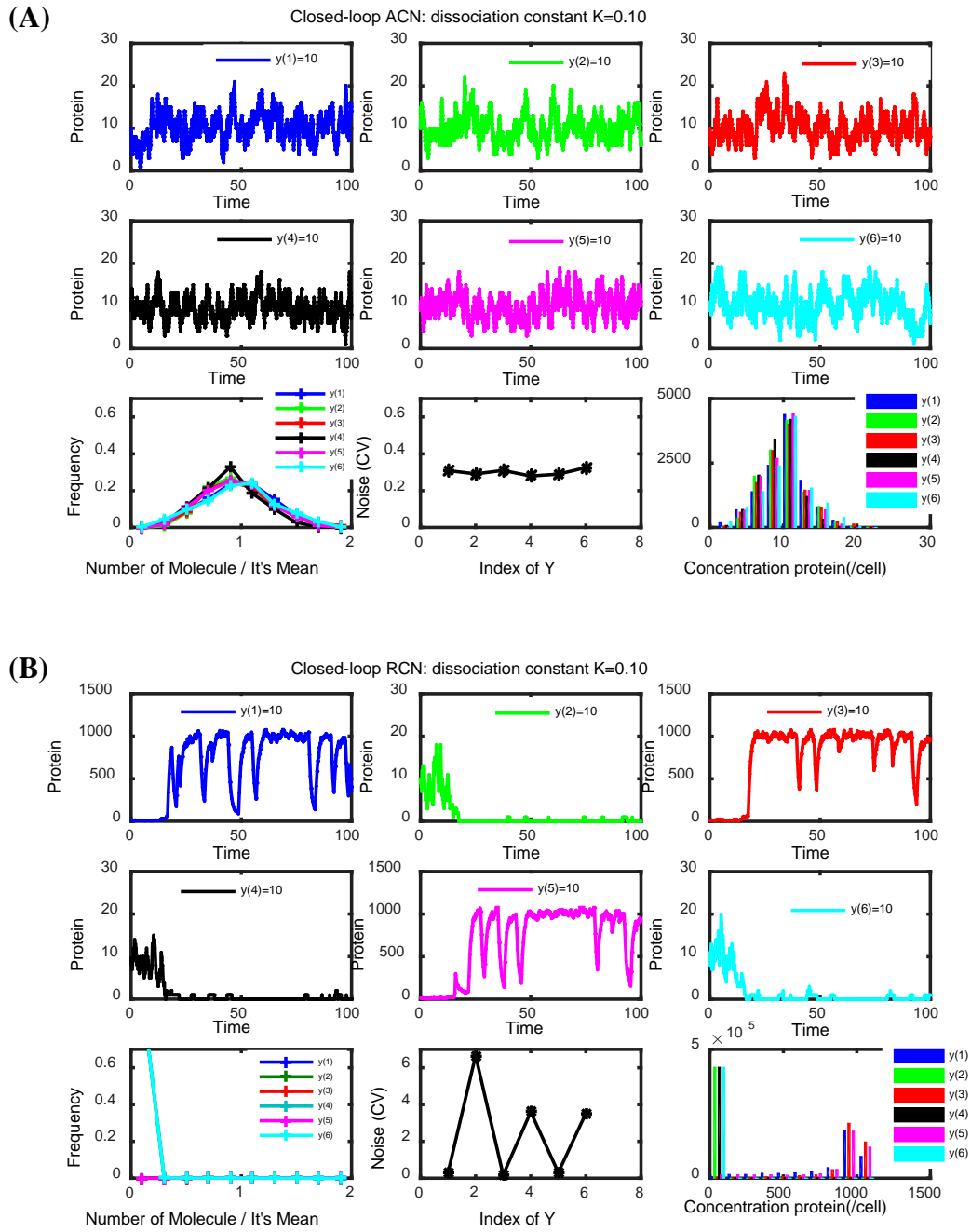


**Fig 3.8. Stochastic simulations of closed-loop system ACN and RCN model for strong dissociation constant.** (A) ACN model, (B) RCN model, stochastic simulation of proteins  $y(1)$ ,  $y(2)$ ,  $y(3)$ ,  $y(4)$ ,  $y(5)$  and  $y(6)$  at dissociation constants  $K = 0.1$  with synthesis rate  $k(1) = k(3) = k(5) = k(7) = K(9) = k(11) = 10$  and degradation rate  $k(2) = k(4) = k(6) = k(8) = k(10) = k(12) = 1$ .

$k(2) = k(4) = k(6) = k(8) = k(10) = k(12) = 1$ . The blue, green, red, black, magenta and cyan appearances indicate  $y(1)$ ,  $y(2)$ ,  $y(3)$ ,  $y(4)$ ,  $y(5)$  and  $y(6)$  proteins respectively with the corresponding fluctuations amplitude, noise amplification cascades, and histograms.

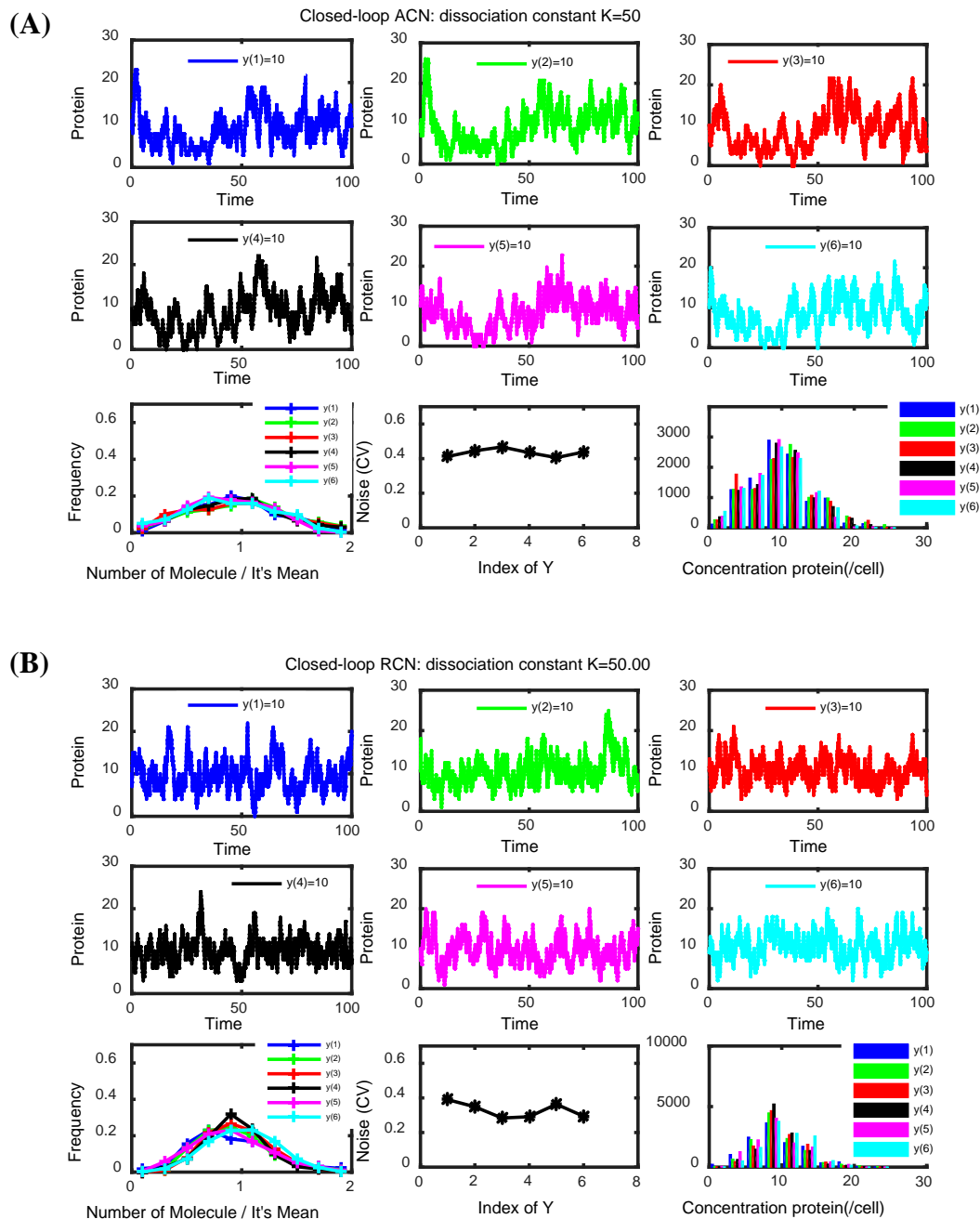


**Fig 3.9. Stochastic simulations of closed-loop system ACN and RCN model for weak dissociation constant.** (A) ACN model, (B) RCN model, stochastic simulation of proteins  $y(1)$ ,  $y(2)$ ,  $y(3)$ ,  $y(4)$ ,  $y(5)$  and  $y(6)$  proteins at dissociation constants  $K = 50$  with synthesis

rate  $k(1) = k(3) = k(5) = k(7) = K(9) = k(11) = 10$  and degradation rate  $k(2) = k(4) = k(6) = k(8) = k(10) = k(12) = 1$ . The blue, green, red, black, magenta and cyan appearances indicate  $y(1)$ ,  $y(2)$ ,  $y(3)$ ,  $y(4)$ ,  $y(5)$  and  $y(6)$  respectively with the corresponding fluctuations amplitude, noise amplification cascades, and histograms.

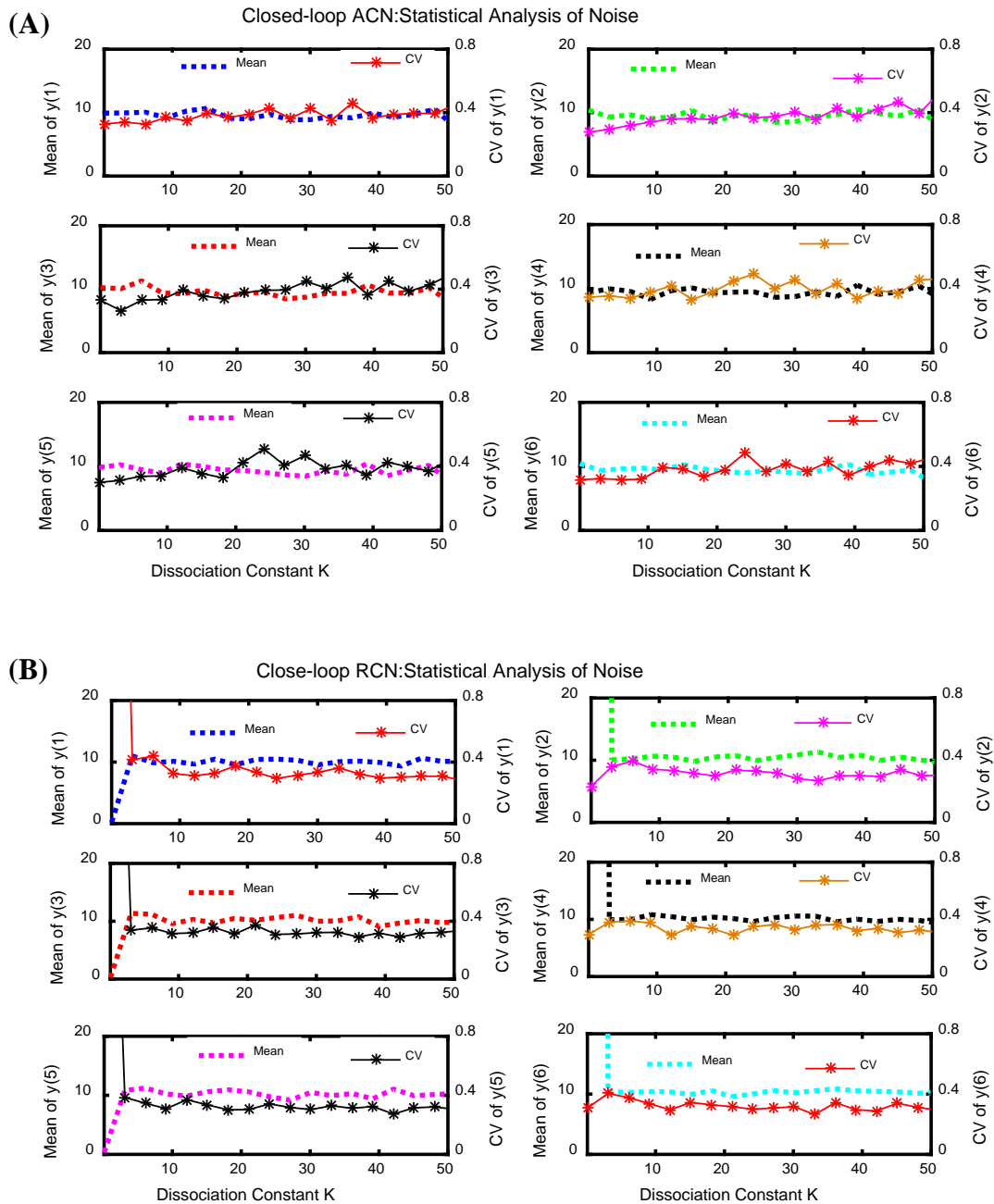


**Fig 3.10. Comparisons of the closed-loop system between ACN and RCN model. (A) ACN model, (B) RCN model, stochastic fluctuations between the ACN and RCN models of proteins**

$y(1)$ ,  $y(2)$ ,  $y(3)$ ,  $y(4)$ ,  $y(5)$  and  $y(6)$ . The means and CVs are simulated with respect to a change in dissociation constants  $K$  while keeping the steady state at a constant level among all the models.

### 3.4 Conclusion

**In open-loop system ACN and RCN model**, noise always amplified from  $y(1)$ ,  $y(2)$  and  $y(3)$  proteins cascade for strong dissociation constant of repressor and vice-versa for strong dissociation constant of activation, when the same concentration of protein level is kept.

**In closed-loop system RCN model**, not only noise always amplified separately among the cascades, but also the  $y(1)$ ,  $y(3)$  and  $y(5)$  are highly stable and others  $y(2)$ ,  $y(4)$  and  $y(6)$  are very poorly stable for strong dissociation constant of repression, when the same concentration of protein level is kept. Noise reduced for weak dissociation constant among the cascades. Consequently, we have shown that closed loops of long repressor cascade increased the noise for strong dissociation constant.

## CHAPTER 4

Gene expression noise can induce stochastic bimodality, even multimodality in deterministically monostable description with non-cooperative binding

### 4.1 Introduction

Bistability gene expression has been studied widely through theoretical analysis and numerically simulations (Shu et al. 2011 and Tian et al. 2006). This system characterized by two stable states under the same external conditions in deterministic approaches while the intrinsic and extrinsic noises can be neglected in the system. To date there are several mechanisms underlying the deterministic bistability gene expression have been identified in the system which consist of a single positive feedback loop with cooperative ligand binding (Wilhelm, 2009 and Cherry et al. 2000), reverse tetracycline transactivation switch in *Saccharomyces cerevisiae* (Becskei et al. 2001), MAPK cascade in *Xenopus* oocytes (Ferrell et al. 1998), bacteriophage  $\lambda$  (Isaacs et al. 2003), lac operon in *Escherichia coli* (Ozbudak et al. 2004), also for multiple feedback loops with cooperativity (Ferrell et al. 2002) and toggle switch between a mutual repression network consisting of LacI and TetR in *E. coli* (Gardner et al. 2000). On the other hand, the distribution of gene products in stochastic approaches that has two maxima is known as bimodal gene expression. Bimodal gene expression is caused by

phenotypic diversity in genetically identical cell populations, and it is critical for population survival in a stochastic fluctuating environment (Acar et al. 2008), some of the bimodal gene expression reported based on geometric construction (Ochab-Marcinek et al. 2010).

The focus of this chapter, to solve the distinct feature among the mutual activation-repression makes the positive feedback system of networks under a stochastic environment. We constructed different types of gene regulatory networks, two-gene regulated mutual activation network (tMAN) comprising p42 MAPK and Cdc2 (Xiong et al. 2003) and cyclinB-Cdc2 and Wee1 (Pomerening et al. 2005) of positive feedback; two-gene regulated mutual repression network (tMRN) consisting of LacI and TetR in *E. coli* (Cherry et al. 2000) makes positive feedback. Here, we have investigated the one gene with respect to another one in both deterministic, stochastic environments by using non-symmetric kinetic parameters to predict the bimodal and multimodal gene expression. Our results suggested that the stochastic bimodality, even multimodality exist in deterministically monostable regime while non-cooperative binding occurred.

## **4.2 Methods and Materials**

### **4.2.1 The regulated tMAN model**

Here, we constructed the simple models of the gene regulatory networks that consist of *two* genes encoding a transcription factor according to the graphical notation (Kurata et al. 2003 and, Kurata et al. 2007), as shown Figs. 4.1-4.2.

The two-gene regulated mutual activation network (tMAN) model consists of  $y(1)$  and  $y(2)$  proteins, thus the syntheses of  $y(1)$  and  $y(2)$  are mutually activated in the way that  $y(2)$  activated  $y(1)$  in a simple binding of non-cooperativity, whereas  $y(1)$  activated  $y(2)$  ultrasensitively, as describe by Hill function (cooperativity in binding); as shown in Fig 1. We employed two types of required outcomes,  $y(1)$  and  $y(2)$  protein synthesis while they are

mutually activated with cooperativity, and only  $y(1)$  protein synthesis while they are mutually activated with non-cooperativity at the steady state level. This model is described by the following mathematical equations:

$$\frac{dy(1)}{dt} = k(1) \cdot \frac{y(2)}{K(1) + y(2)} - k(2) \cdot y(1) \quad (4.1)$$

$$\frac{dy(2)}{dt} = k(3) \cdot \frac{y(1)^n}{K(2)^n + y(1)^n} - k(4) \cdot y(2) \quad (4.2)$$

where the employed parameters are described in Table 4.1.

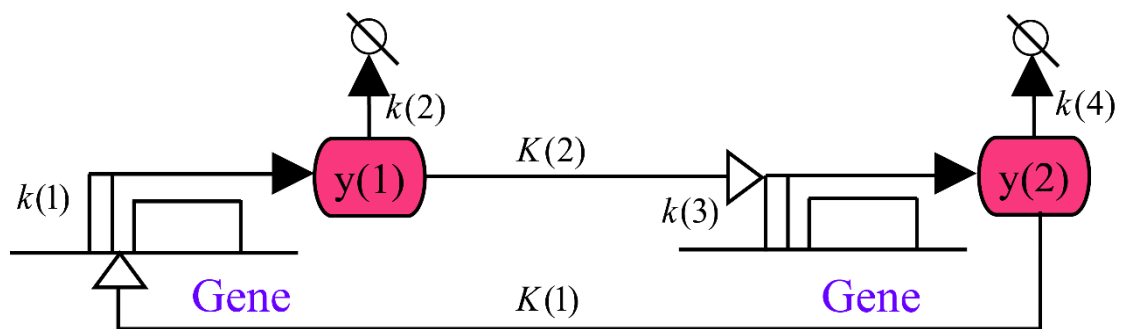


**Fig 4.1. The network map of the tMAN model.** This mutual activation network consists of  $y(1)$  and  $y(2)$  proteins synthesis with the first-order degradation

**Table 4.1.** List of kinetic parameters used in the tMAN and tMRN models

Kinetic parameters	Definition
$k(1), k(3)$	protein synthesis rate constants
$k(2), k(4)$	degradation rate constants
$K(1), K(2)$	dissociation constant
$n$	Hill coefficient

## 4.2.2 The regulated tMRN model

The two-gene regulated mutual repression network (tMRN) model consists of  $y(1)$  and  $y(2)$  proteins, thus the syntheses of  $y(1)$  and  $y(2)$  are mutually repressed in the way that  $y(2)$  repressed  $y(1)$  in a simple binding of non-cooperativity, whereas  $y(1)$  repressed  $y(2)$  ultrasensitively, as describes by Hill function (cooperativity in binding); as shown in Fig.4.3. Also, we employed two types of required outcomes which are  $y(1)$  and  $y(2)$  protein synthesis while they are mutually repressed with cooperativity; only  $y(1)$  protein synthesis while they are mutually repressed with non-cooperativity at the steady state level. This model is described by the following mathematical equations:

$$\frac{dy(1)}{dt} = k(1) \cdot \frac{K(1)}{K(1) + y(2)} - k(2) \cdot y(1) \quad (4.3)$$

$$\frac{dy(2)}{dt} = k(3) \cdot \frac{K(2)^n}{K(2)^n + y(1)^n} - k(4) \cdot y(2) \quad (4.4)$$

where the employed parameters are described in Table 4.1.

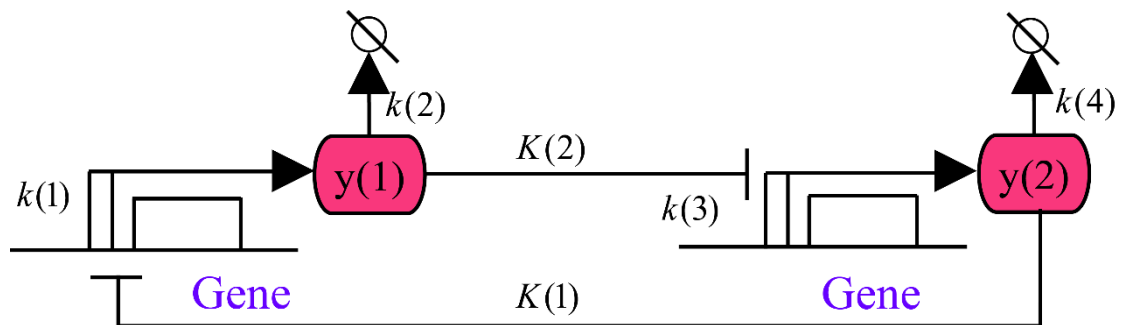


**Fig 4.2. The network map of the tMRN model.** This mutual repression network consists of  $y(1)$  and  $y(2)$  proteins synthesis with the first-order degradation

The Gillespie and Tau-Leap stochastic algorithm was used to perform the stochastic simulation (Gillespie 1977). The MATLAB (Mathworks) was employed for this simulation results.

### **4.3 Results and discussion**

We have investigated the noise effect just before our proposed of genetic network models at the steady state level when the value of hill coefficient  $n = 1$  (non-cooperative binding). In which case we employed the stochastic activities of one gene with respect to another gene when the corresponding kinetic parameters are non-symmetric at the steady state level.

#### **4.3.1 Robustness of bimodal, multimodal in the tMAN model**

We examined the tMAN model at non-cooperative binding i.e. hill coefficient  $n = 1$  and of  $y(1)$  protein was an outcome while changing the degradation rate constant of  $y(2)$ ,  $k(4) = 0.0008$ ,  $k(4) = 0.008$  and  $k(4) = 0.8$  at fixed dissociation constants of  $K(1) = 5$ ,  $K(2) = 1$  and where the other corresponding kinetic parameters were set as fixed-synthesis rate  $k(1) = 30$ ,  $k(3) = 0.001$  with a degradation rate of  $y(1)$ ,  $k(2) = 0.1$ . The deterministic simulations showed the only one stable state i.e. monostable position of  $y(1)$  protein synthesis in Fig. 4.3 (A). But, the steady-state stochastic simulation of  $y(1)$  protein showed one stable, bistable and multistable states as well as the unimodal, bimodal and multimodal distribution in Fig. 4.3 (B).

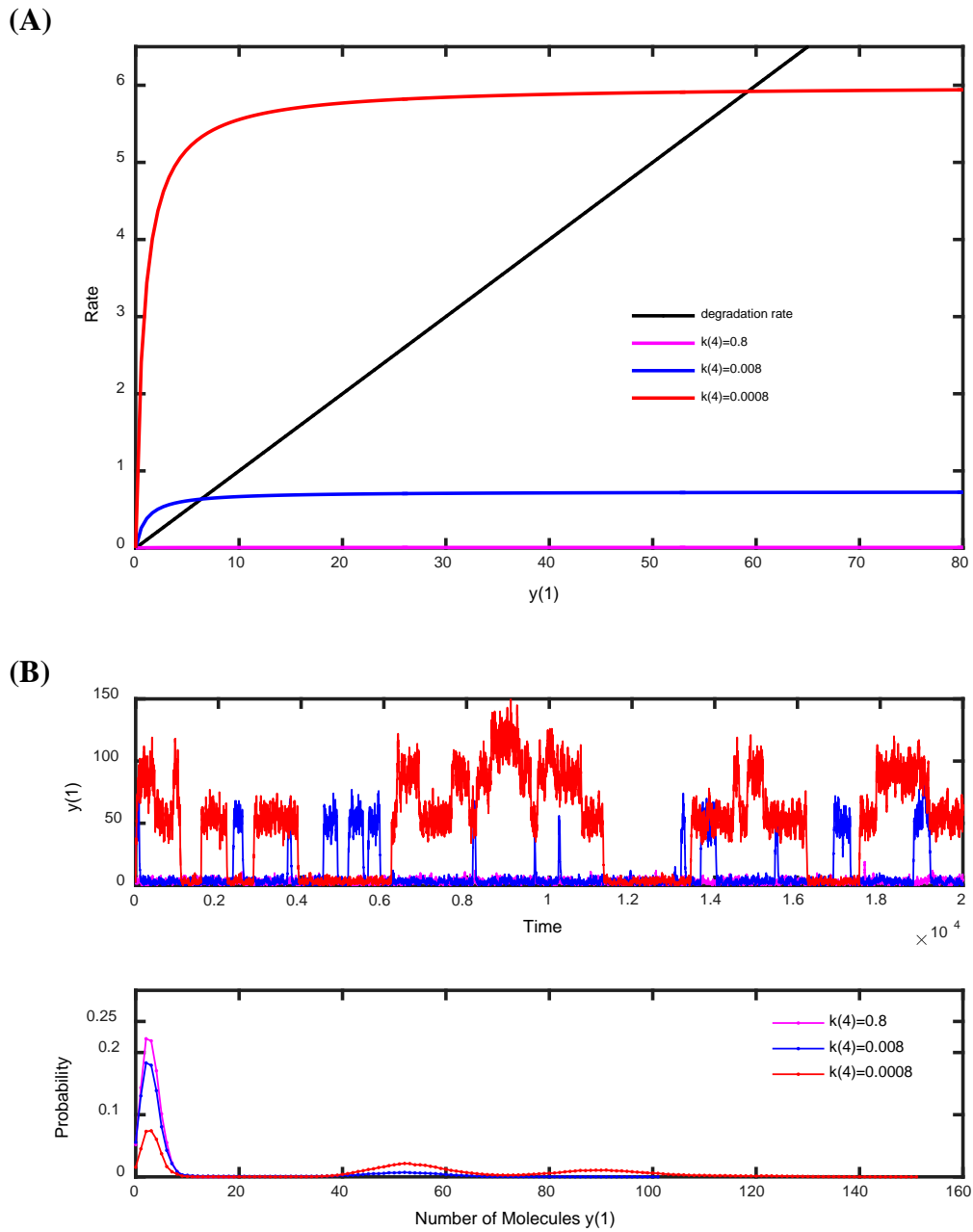


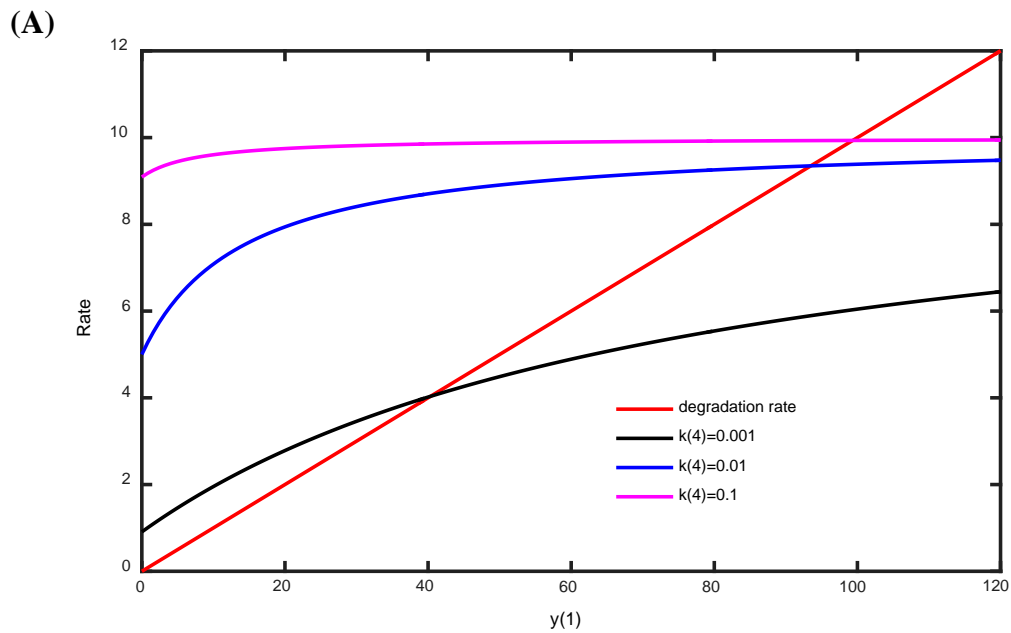
**Fig 4.3. Deterministic and stochastic simulations of the tMAN model for non-cooperative binding**

(A) Equilibrium points of  $y(1)$  protein at hill coefficient  $n = 1$  and different dissociation constants  $K(1) = 5$ ,  $K(2) = 1$  with synthesis rate  $k(1) = 30$ ,  $k(3) = 0.001$  and degradation rate  $k(2) = 0.1$ . The black lines indicate the degradation and red, blue and magenta lines indicates the synthesis of  $y(1)$  protein at the degradation rate constants  $k(4) = 0.0008$ ,  $k(4) = 0.008$  and

$k(4) = 0.8$  respectively. (B) Stochastic simulations of  $y(1)$  protein with corresponding probability distributions.

### 4.3.2 Robustness of bimodal, multimodal in the tMRN model

We investigated the tMRN model at non-cooperative binding i.e. hill coefficient  $n = 1$  and of  $y(1)$  protein was an outcome while changing the degradation rate constant of  $y(2)$ ,  $k(4) = 0.001$ ,  $k(4) = 0.01$  and  $k(4) = 0.1$  at dissociation constants of  $K(1) = 1$ ,  $K(2) = 7$  and where the other corresponding kinetic parameters were set as synthesis rate  $k(1) = 10$ ,  $k(3) = 0.01$  with a degradation rate of  $y(1)$ ,  $k(2) = 0.1$ . The deterministic simulations showed the only one stable state i.e. monostable position of  $y(1)$  protein synthesis in Fig. 4.4 (A). But, the corresponding steady-state stochastic simulation of  $y(1)$  protein showed one stable, bistable and multistable states as well as the unimodal, bimodal and multimodal distribution in Fig. 4.4 (B-C).



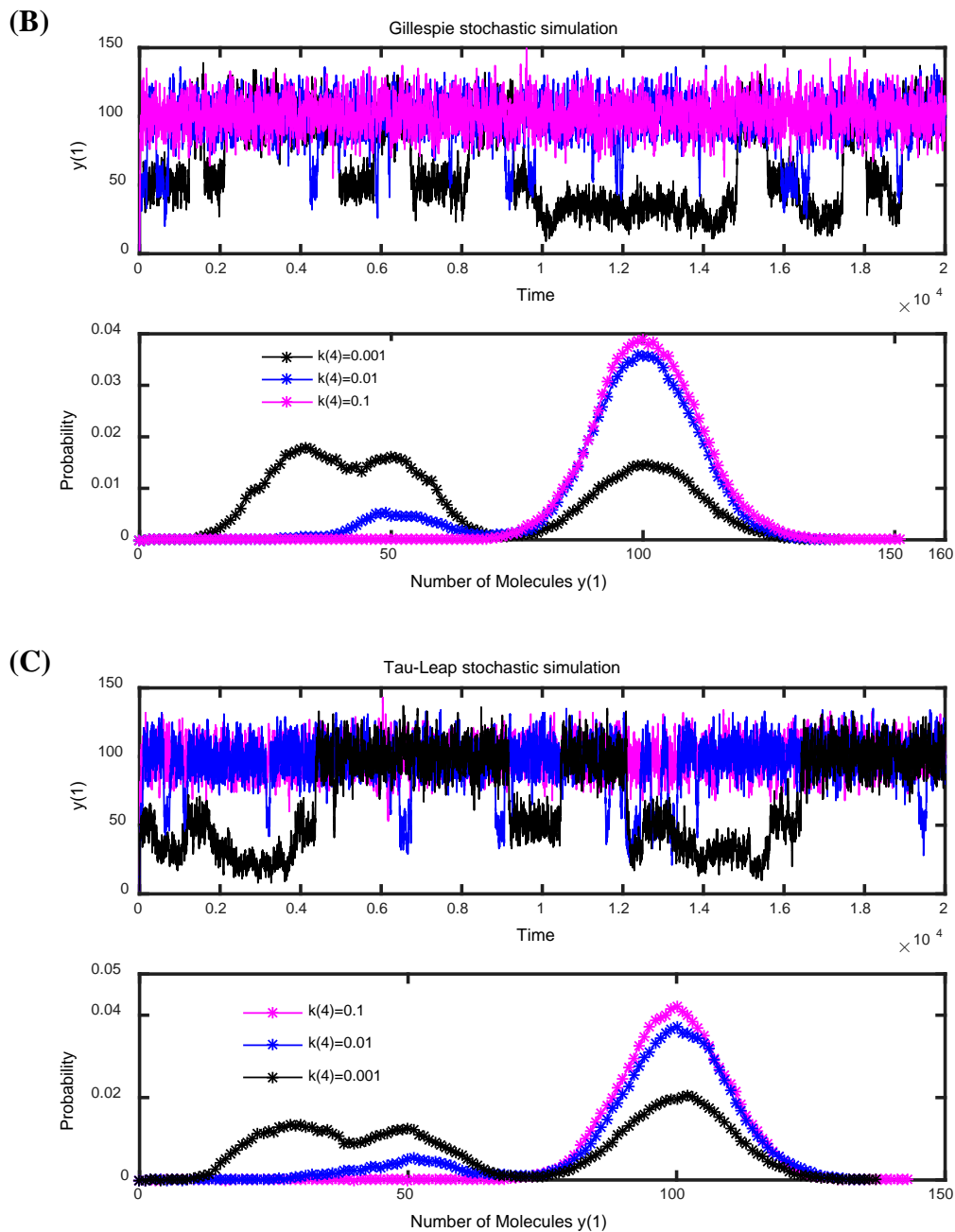


**Fig 4.4. Deterministic and stochastic simulations of the tMRN model for non-cooperative binding**

(A) Equilibrium points of  $y(1)$  protein at hill coefficient  $n = 1$  and different dissociation constants  $K(1) = 1$ ,  $K(2) = 7$  with synthesis rate  $k(1) = 10$ ,  $k(3) = 0.01$  and degradation rate  $k(2) = 0.1$ . The red lines indicate the degradation and black, blue and magenta lines indicates the synthesis of  $y(1)$  protein at the degradation rate constants  $k(4) = 0.001$ ,  $k(4) = 0.01$  and

$k(4) = 0.1$  respectively. (B) Stochastic simulations of  $y(1)$  protein with corresponding probability distributions. (C) Tau-Leap stochastic simulations of  $y(1)$  protein with corresponding probability distributions.

#### **4.4 Discussion**

We analyzed the mechanism of how mutual activation and repression networks generate a robust noise induced bistable (bimodal), multistable (multimodal) of this gene regulatory networks in deterministic and stochastic respectively approaches at the steady state level. The tMAN and tMRN model demonstrated the unimodal, bimodal and multimodal distribution with corresponding deterministic simulation showed monostable when changing the degradation rate constant of  $y(2)$  proteins in Figs. (4.3, 4.4). These distributions peaks were not coincided with the corresponding equilibrium points of proteins synthesis except for unimodal. Also, the lower peak coincided with the monostable point in the stochastic bimodal system and the middle peak coincided with the monostable point for the stochastic multimodal system. Therefore, exhibited the stochastic bimodality, even multimodality in these two lower corresponding deterministically monostable regime without cooperative binding as a result based on the discreteness amplification of the molecular concentration.

A mutual activation network that comprises two protein kinases p42 MAPK and Cdc2 (Xiong et al. 2003) and a mutual repression that consists of cI and Cro proteins (Casadesus et al. 2002) have shown stochastic bimodality, even multimodality exist in deterministically monostable regime while non-cooperative binding.

#### **4.5 Conclusion**

The results were generalized for both mutual activation and repression networks. We used non-symmetric kinetics parameters set for a range of biologically relevant conditions thus

shown stochastic bimodality, even multimodality exist in deterministically monostable regime while non-cooperative binding. Bimodality, multimodality are observed not only for parameter values corresponding to deterministic but also beyond it occurred as the discreteness amplification of the molecular concentration. Our results expected to have significant implications on the dynamical behavior of gene in cell populations.

## CHAPTER 5

# Mathematical comparison of memory functions between mutual activation and repression networks in a stochastic environment

The work in this chapter has been accepted in *Journal of Theoretical Biology*

### 5.1. Introduction

Systems biology and theoretical biology have revealed the mechanisms by which a biochemical network generates a variety of functions such as switching, amplification, adaptation, pulse generation, oscillation and memory (Kurata et al., 2014), allowing biologists to design useful genetic circuits based on this rational understanding of biological networks (Tan et al., 2009; Tabor et al., 2009; Auslander et al., 2012; Daniel et al., 2013; Ajo-Franklin et al., 2007; Basu et al., 2005; Elowitz and Leibler, 2000; Moon et al., 2012). Feedback loops are common control mechanisms (Brandman and Meyer, 2008): a negative feedback loop generates adaptation and oscillation (Elowitz and Leibler, 2000), and a positive feedback loop generates amplifiers, bistable switches (Hasty et al., 2000) and memory (Ajo-Franklin et al., 2007). For example, genetic circuits with a two-molecule input have been engineered to execute sophisticated computational logic functions (Tabor et al., 2009; Auslander et al., 2012; Daniel et al., 2013; Moon et al., 2012), and genetic logic gates capable of generating a Boolean function play critically important roles in synthetic biology. Each Boolean circuit integrates a two-molecule

input into a digital ON/OFF expression decision, following the processing logic of NOT, AND, NAND and N-IMPLY gates. Other noteworthy developments include an AND gate designed on the basis of the  $\sigma^{54}$ -dependent hrpR/hrpS hetero-regulation module in *Escherichia coli* (Wang et al., 2011). The SynBioLGDB database provides the synthetic biology community with a useful resource for efficient browsing and visualization of genetic logic gates (Wang et al., 2015).

Memory plays pivotal roles in cellular development, survival and growth (Xiong and Ferrell, 2003; Shopera et al., 2015; Freeman, 2000), and is a ubiquitous function embedded in complex gene regulatory networks and signal transduction pathways (Cheng et al., 2008; Casadesus and D'Ari, 2002; Burrill and Silver, 2010). Cellular memory indicates that transient signals lock cells into one of two or more regulatory states. Common features of memory mechanisms have been experimentally and theoretically revealed to be based on positive feedback loops (Xiong and Ferrell, 2003; Shopera et al., 2015; Cheng et al., 2008; Kim and Ferrell, 2007; Acar et al., 2005; Gardner et al., 2000; Ferrell, 2002). An ultrasensitive positive feedback loop is a typical approach for generating two stable states that can exhibit irreversibility or hysteresis (Xiong and Ferrell, 2003; Kim and Ferrell, 2007; Acar et al., 2005). It is a building block of synthetic gene circuits and is useful for rational design in biotechnology, biocomputing, and in gene therapy (Cherry and Adler, 2000; Becskei et al., 2001; Alon, 2007). The bistable modules consisting of two genes have extensively been investigated. Mutual activation networks comprises p42 MAPK and Cdc2 (Xiong and Ferrell, 2003), cyclinB-Cdc2 and Wee1 (Pomerening et al., 2005), and a mutual repression network consists of LacI and TetR in *E. coli* (Gardner et al., 2000). Mutual repression of the two repressors cI and Cro provided a lysis-lysogen decision-making module in a bacteriophage  $\lambda$  switch (Casadesus and D'Ari, 2002). Although these mutual activations and repressions were shown to form a positive feedback

loop to generate a bistable function, to our knowledge they have not been compared with the intent of identifying functional differences. The quantitative or mathematical characterization of these loops will allow selection of a bistable or memory module optimal for the rational design of a specific function, as well as an understanding of how different types of a positive feedback loop have evolved under a given environment.

Gene expression is a complex and nonlinear system involving numerous components within a cell and this system is continuously exposed to stochastic fluctuations (McAdams and Arkin, 1997; Ozbudak et al., 2002; Elowitz et al., 2002; Blake et al., 2003; Pedraza and van Oudenaarden, 2005; Eldar and Elowitz, 2010). Noise in gene expression is provided by intrinsic fluctuations such as the number of molecules per cell and the uncertainty of kinetic parameters, as well as by extrinsic perturbations from upstream regulators (Pedraza and van Oudenaarden, 2005). The intrinsic and extrinsic stochastic behaviors are essential sources of the noise observed in cellular events (McAdams and Arkin, 1997), with translational efficiency being the predominant source of increased noise (Ozbudak et al., 2002). A negative feedback loop suppresses noise, whereas a positive feedback loop can increase the amplitude of noise (Elowitz et al., 2002), leading to increased cell–cell variability in the target gene output (Blake et al., 2003).

Recently noise has been reported to induce multimodality or stochastic memory in a wide class of regulatory networks whose corresponding deterministic description lacks bistability (Thomas et al., 2014). On the other hand, noise can drive a bistable system to undergo stochastic transitions between multiple states, which impair memory functions. The ability to sustain memory functions under noise is a key property of cellular systems (Cheng et al., 2008).

A memory module needs to sustain the states induced by the transient signals for a long time. It is important to address the mechanism by which cellular memory is sustained in the presence of stochasticity.

In this study we focus on a typical property of the bistable networks achieved by a positive feedback loop with ultrasensitivity. We aim to identify the feature distinguishing mutual activation and repression networks under a stochastic environment. To this end, we constructed two gene regulatory networks, namely, a regulated mutual activation network (MAN) and a regulated mutual repression network (MRN), in which the input signal works as a triggering stimulus for the expression of target genes. Numerical and theoretical comparison of the deterministic and stochastic models allowed identification of essential differences in the memory functions between these competitive models.

## 5.2. Methods

### 5.2.1. Competitive network models

We constructed two gene regulatory networks, each of which consists of two genes encoding a transcription factor, according to graphical notation (Kurata et al., 2003; Kurata et al., 2007), as shown **Fig. 5.1**. The regulated mutual activation network (MAN) consists of  $y(1)$ ,  $y(2)$  and  $y(3)$  proteins, as shown in **Fig. 5.1A**. The MAN shows a memory function. Signal-induced  $y(1)$  activates the synthesis of  $y(2)$  and  $y(3)$ , in which  $y(2)$  and  $y(3)$  are mutually and cooperatively activated. Once the input signal activates the synthesis of  $y(2)$  and  $y(3)$ , their activated protein levels are locked ON or sustained after the input signal disappears. This model is described by:

$$\frac{dy(1)}{dt} = k(1).S - k(2).y(1) \quad (5.1)$$

$$\frac{dy(2)}{dt} = b + k(3).\frac{y(1)}{y(1) + K(1)} + k(4).\frac{y(3)^n}{y(3)^n + K(2)^n} - k(5).y(2) \quad (5.2)$$

$$\frac{dy(3)}{dt} = b + k(6).\frac{y(1)}{y(1) + K(3)} + k(7).\frac{y(2)^n}{y(2)^n + K(4)^n} - k(8).y(3) \quad (5.3)$$

where the employed parameters are described in **Table 5.1**. We used a very low rate constant of  $b = 0.01$  for basal synthesis of the activators to prevent protein synthesis from being shut down (Cheng et al., 2008).

The regulated mutual repression network (MRN) consists of  $y(1)$ ,  $y(2)$  and  $y(3)$  proteins, as shown in **Fig. 5.1B**. An input signal induces the synthesis of  $y(1)$ , which activates the synthesis of  $y(2)$  and represses that of  $y(3)$ . The synthesis of  $y(2)$  and  $y(3)$  is mutually and cooperatively repressed. Consequently, the two protein levels can be locked ON and OFF even after the input signal disappears. This model is described by:

$$\frac{dy(1)}{dt} = k(1).S - k(2).y(1) \quad (5.4)$$

$$\frac{dy(2)}{dt} = k(3).\frac{y(1)}{y(1) + K(1)} + k(4).\frac{K(2)^n}{y(3)^n + K(2)^n} - k(5).y(2) \quad (5.5)$$

$$\frac{dy(3)}{dt} = k(6).\frac{K(3)}{y(1) + K(3)} + k(7).\frac{K(4)^n}{y(2)^n + K(4)^n} - k(8).y(3) \quad (5.6)$$

where the employed parameters are described in **Table 5.1**.

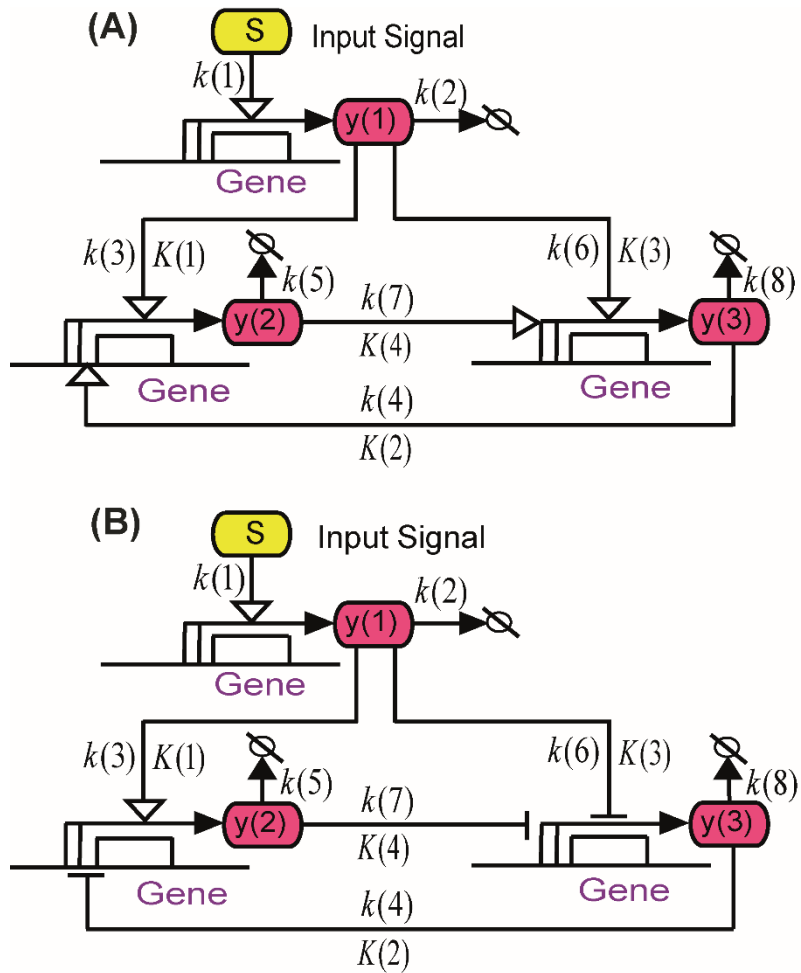


**Fig. 5.1 Two competitive network maps**

(A) The MAN. Protein  $y(1)$  acts as a switch for mutual activation of proteins  $y(2)$  and  $y(3)$ . (B) The MRN. Protein  $y(1)$  acts as a switch for mutual repression of proteins  $y(2)$  and  $y(3)$ .

**Table 5.1 List of kinetic parameters used in gene regulatory networks**

Kinetic parameters	Definition
$k(1), k(3), k(4), k(6), k(7)$	protein synthesis rate constants
$k(2), k(5), k(8)$	degradation rate constants
$K(1), K(2), K(3), K(4)$	dissociation constants of activators/repressors
$n$	Hill coefficient

### 5.2.2. Mathematical comparison

To set a sound basis for comparison between the two competitive models, their equivalence should be guaranteed with respect to their function and corresponding kinetics. It is important to identify different structures between the competitive models and to understand the characteristics of the structures within each model. This is very much in the spirit of mathematically controlled comparisons (Alves and Savageau, 2000; Kurata et al., 2006). To compare a specific function between the two competitive models, we fix or conserve the other functions of the models while reducing the search space by setting the corresponding kinetic parameters to the same values. The network structure between the MAN and MRN is the same, except that activators are replaced by repressors in the MRN. The interactions between the two components of  $y(2)$  and  $y(3)$  within each model show a symmetric structure.

An objective of the proposed models is to sustain the memory function for an extended period of time. The memory function is characterized by the persistence of gene expression after the input stimulus disappears. Since the models show bistability, they have two steady states: a

high level and a low level. For the MAN, both the high and low steady states of  $y(2)$  and  $y(3)$  are readily set to the same levels, as shown in **Table 5.2**. For the MRN, the steady-state levels of  $y(2)$  and  $y(3)$  are always opposite: when the steady-state level of  $y(2)$  is high; that of  $y(3)$  is low. When the high steady-state level of  $y(2)$  in the MRN is set to the same level as that in the MAN, the low steady-state level of  $y(2)$  in the MRN cannot be set to the same level as that in the MAN, as shown in **Appendix A** and **B**. Thus, we conserved the high steady-state level of  $y(2)$  between the MAN and MRN. In addition, to reduce the search in the parameter space, we set the corresponding parameters between the two models to the same values and set the corresponding parameters within each model to the same values, as shown in **Table 5.3**. To reveal the difference in memory function between the two models, we selected two parameters responsible for gene regulation: the Hill coefficient ( $n$ ), and the dissociation constant ( $K(2) = K(4)$ ). These two parameters indicate the cooperativity of gene expression by activators and repressors and their binding strengths for each other.

**Table 5.2 Steady-state levels of gene expression in the MAN and MRN models**

	MAN	MRN
Conserved function within each network	The low and high steady-state levels of $y(2)$ and $y(3)$	The high steady-state levels of $y(2)$ and $y(3)$
Conserved function between the MAN and MRN models	The high steady-state levels of $y(2)$ and $y(3)$ The low steady-state cannot be kept at the same level between the MAN and MRN networks.	

**Table 5.3 Corresponding kinetic parameters for the two competitive models**

	MAN	MRN
Corresponding parameters within each network	$k(3) = k(6) = 18.1$ $k(4) = k(7)$ $k(5) = k(8) = 0.8$ $K(1) = K(3) = 9$ $K(2) = K(4) = 43$	$k(3) = k(6) = 18.1$ $k(4) > k(7), k(7) = 43.1$ $k(5) = k(8) = 0.8$ $K(1) = K(3) = 9$ $K(2) = K(4) = 43$
Corresponding parameters between the MAN and MRN models	$k(1) = 100 \quad k(2) = 1$ $k(3) \quad k(5) \quad k(6) \quad k(8)$ $K(1) \quad K(2) \quad K(3) \quad K(4)$	

### 5.2.3. Time-course simulation of memory

The deterministic and stochastic time courses of  $y(1)$ ,  $y(2)$  and  $y(3)$  were simulated from time 0 to 1,000. Signal  $S$  was input from time 250 to 500. The memory is divided into deterministic memory and stochastic memory. In deterministic memory, the protein levels are sustained after signal  $S$  disappears at 500. The stochastic time-course of  $y(2)$  and  $y(3)$  during the period from 500 to 1,000 is simulated by the Gillespie stochastic simulation algorithm (Gillespie, 1977) to determine whether the memory is sustained or persistent. In this analysis, stochastic persistent memory was defined that sustains a gene expression level after an input signal disappears. This term can be distinguished from widely-used stochastic memory showing frequent transitions between two states and was effective in characterizing the memory persistence. In this simulation, the requirement of the stochastic persistent memory was empirically defined as the

requirement that the sustained expression of  $y(2)$  and  $y(3)$  during the period of time from 500 to 1,000 after the signal disappears is more than 8 times obtained from 10 repetitions of simulations.

#### 5.2.4. Potential and probability density

To theoretically perform deterministic and stochastic potential analysis, we converted the reaction rate equations (Eqs. (5.1-5.3)) into one-variable rate equations  $f_{MAN2}(y)$  and  $f_{MAN3}(y)$  by the quasi-steady-state approximation (**Appendix C**). In the same manner, the reaction rate equations (Eqs. (5.4-5.6)) were converted into  $f_{MRN2}(y)$  and  $f_{MRN3}(y)$  (**Appendix D**). Here, we illustrated how a one-variable equation  $f_{MAN2}(y)$  is given under a stochastic environment by:

$$\frac{dy}{dt} = f_{MAN2}(y) = b + k(4) \cdot \frac{[\{b + k(7) \cdot \frac{y^n}{y^n + K(2)^n}\} \cdot \frac{1}{k(8)}]^n}{[\{b + k(7) \cdot \frac{y^n}{y^n + K(2)^n}\} \cdot \frac{1}{k(8)}]^n + K(2)^n} - k(5) \cdot y \quad (5.7)$$

This equation can be described by the birth-and-death stochastic processes (Cheng et al., 2008, Scott et al., 2007):

$$W_{birth}(y) = b + k(4) \cdot \frac{[\{b + k(7) \cdot \frac{y^n}{y^n + K(2)^n}\} \cdot \frac{1}{k(8)}]^n}{[\{b + k(7) \cdot \frac{y^n}{y^n + K(2)^n}\} \cdot \frac{1}{k(8)}]^n + K(2)^n} \quad (5.8)$$

$$W_{death}(y) = k(5) \cdot y \quad (5.9)$$

The corresponding chemical master equation was given by:

$$\frac{\partial P(y,t)}{\partial t} = W_{birth}(y-1)P(y-1,t) + W_{death}(y+1)P(y+1,t) - \{W_{birth}(y) + W_{death}(y)\}P(y,t) \quad (5.10)$$

where  $P(y,t)$  was the probability density of protein concentration  $y$ . Next, the chemical master equation was transformed into the Fokker-Planck equation (Gillespie, 2000, Gardiner, 2009; Cheng et al., 2008, Scott et al., 2007):

$$\frac{\partial P(y,t)}{\partial t} = -\frac{\partial}{\partial x}[A(y)P(y,t)] + \frac{1}{2}\frac{\partial^2}{\partial x^2}[B(y)P(y,t)] \quad (5.11)$$

where

$$A(y) = b + k(4) \cdot \frac{[b + k(7) \cdot \frac{y^n}{y^n + K(2)^n}] \cdot \frac{1}{k(8)}]^n}{[b + k(7) \cdot \frac{y^n}{y^n + K(2)^n}] \cdot \frac{1}{k(8)}]^n + K(2)^n} - k(5) \cdot y \quad (5.12)$$

The noise function is given by:

$$B(y) = b + k(4) \cdot \frac{[b + k(7) \cdot \frac{y^n}{y^n + K(2)^n}] \cdot \frac{1}{k(8)}]^n}{[b + k(7) \cdot \frac{y^n}{y^n + K(2)^n}] \cdot \frac{1}{k(8)}]^n + K(2)^n} + k(5) \cdot y \quad (5.13)$$

In the same manner, the Fokker-Planck equations of the four one-variable equations including

$f_{MAN2}(y)$  were solved under the following conditions (**Appendix C and D**):

$$A(y) = \begin{cases} f_{MAN2}(y) & \text{for } y = y(2) \\ f_{MAN3}(y) & \text{for } y = y(3) \end{cases} \quad \text{for the MAN model} \quad (5.14)$$

$$A(y) = \begin{cases} f_{MRN2}(y) & \text{for } y = y(2) \\ f_{MRN3}(y) & \text{for } y = y(3) \end{cases} \quad \text{for the MRN model} \quad (5.15)$$

and the noise functions were given by:

$$B(y) = \begin{cases} g_{MAN2}(y) & \text{for } y = y(2) \\ g_{MAN3}(y) & \text{for } y = y(3) \end{cases} \quad \text{for the MAN model} \quad (5.16)$$

$$B(y) = \begin{cases} g_{MRN2}(y) & \text{for } y = y(2) \\ g_{MRN3}(y) & \text{for } y = y(3) \end{cases} \quad \text{for the MRN model} \quad (5.17)$$

Finally, we consider the stochastic potential analysis. The limit of  $P(y, t)$  as  $t \rightarrow \infty$  yields  $P_{st}(y)$ , the stationary probability density function of  $y$  (Scott et al., 2007; Cheng et al., 2008), which is given by:

$$P_{st}(y) = \frac{N_c}{B(y)} \exp\left[2 \int^x \frac{A(z)}{B(z)} dz\right] \quad (5.18)$$

where  $N_c$  is the normalization constant. Eq. (5.18) can be recast in the form:

$$P_{st}(y) = N_c e^{-2\Phi_s(y)} \quad (5.19)$$

where

$$\Phi_s(y) = \frac{1}{2} \ln[B(y)] - \int^y \frac{A(z) dz}{B(z)} \quad (5.20)$$

is called the stochastic potential of  $f(y)$  (Gardiner, 2009; Risken and Frank, 1996; Scott et al., 2007).

### 5.2.5. Mean first-passage time analysis

The robustness or persistency of steady states is estimated in the presence of noise. The persistency of the steady state of a stochastic system can be estimated by the mean first-passage

time (MFPT). An equilibrium point can exit from its minimum potential due to the effect of noise. The exit time depends on the specific realization of the random process and it is known as the first passage time. The MFPT is the average of the first passage times over many realizations. In the context of anticipating phase shifts, the MFPT provides a useful characterization of the time-scale on which a phase transition is likely to happen.

Let us consider  $y_l^{st}$  and  $y_u^{st}$  ( $y_l^{st} < y_u^{st}$ ) as two steady states corresponding to a low and a high protein concentration, respectively, separated by the unstable steady state defining the potential barrier  $y_b^{un}$  (i.e., the unstable equilibrium point). The basin of attraction of the state  $y_u^{st}$  extends from  $y_b^{un}$  to  $+\infty$ , as it is to the right of  $y_l^{st}$ . Let  $T(y)$  be the MFPT to state  $y_b^{un}$  starting at  $y > y_b^{un}$ .  $T(y)$  satisfies the following ordinary differential equation (Gardiner, 2009, Drury, 2007, Sharma et al., 2016):

$$A(y)\frac{\partial T(y)}{\partial y} + \frac{1}{2}B(y)\frac{\partial^2 T(y)}{\partial y^2} = -1 \quad (5.21)$$

with boundary conditions:

$$T(y_b^{un}) = 0 \text{ and } \frac{\partial T(+\infty)}{\partial y} = 0 \quad (5.22)$$

By solving Eqs. (5.21-5.22), the MFPTs of  $y_u^{st}$  and  $y_l^{st}$ :  $T_U(y_u^{st})$  and  $T_L(y_l^{st})$  are calculated to state  $y_b^{un}$  for the basin of attraction of the state  $y_u^{st}$  extending from  $y_b^{un}$  to  $+\infty$  and for the basin of attraction of the state  $y_l^{st}$  which extends from 0 to  $y_b^{un}$ , respectively, as follows:

$$T_L(y_l^{st}) = 2 \int_{y_l^{st}}^{y_b^{un}} \frac{1}{\Psi(x)} dx \int_0^x \frac{\Psi(z)}{B(z)} dz \quad (5.23)$$

$$T_U(y_u^{st}) = 2 \int_{y_b^{un}}^{y_u^{st}} \frac{1}{\Psi(x)} dx \cdot \int_x^{\infty} \frac{\Psi(z)}{B(z)} dz \quad (5.24)$$

where

$$\Psi(y) = \exp\left(\int_{y_0}^y \frac{2A(w)}{B(w)} dw\right) \quad (5.25)$$

with  $y_0 = 0$  for the  $y_u^{st} \rightarrow y_l^{st}$  transition and  $y_0 = y_b^{un}$  for the  $y_l^{st} \rightarrow y_u^{st}$  transition.

### 5.2.6. Theoretical comparison between the MAN and MRN models

For theoretical analysis, we converted the reaction rate equations of the MAN and MRN models into the one-variable rate equations (**Appendix C** and **D**). The one-variable rate equations were used to analyze the stochastic potential profile and estimate the MFPTs of the low and high steady-state levels.  $T_L(y(2)_l^{st})$ ,  $T_U(y(2)_u^{st})$ ,  $T_L(y(3)_l^{st})$  and  $T_U(y(3)_u^{st})$  of the MAN were calculated by Eqs. (23-25).  $T_L(y(2)_l^{st})$ ,  $T_U(y(2)_u^{st})$ ,  $T_L(y(3)_l^{st})$  and  $T_U(y(3)_u^{st})$  of the MRN were calculated in the same manner. A high value of the MFPT of a steady-state protein level means that the level is sustained for a longer time, whereas a low value indicates that the protein level quickly transitions to another level.

### 5.2.7. Calculation

MATLAB (Mathworks) was used for all the calculations.

## 5.3. Results

### 5.3.1. MAN-enhanced memory function

We investigated the MAN at a Hill coefficient of  $n = 2$  and at the different dissociation constants of  $K(2) = K(4) = 46$  and  $K(2) = K(4) = 43$  the other corresponding kinetic parameters were set as shown in **Table 5.3**. The steady-state levels of  $y(2)$  and  $y(3)$  were set to be the same (**Appendix A**). The dynamics of the MAN was simulated according to the Gillespie stochastic method. As shown in **Fig. 5.2A**, when signal  $S$  was input from time 250 to 500,  $S$ -induced  $y(1)$  activated  $y(2)$  and  $y(3)$ . The dynamic behaviors of  $y(2)$  and  $y(3)$  were identical because the structurally-corresponding parameters between  $y(2)$  and  $y(3)$  within the model were set to be the same. Proteins  $y(2)$  and  $y(3)$  showed memory effects after 500 by mutual activation, and a high level of  $y(2)$  and  $y(3)$  was sustained after  $S$  disappeared. The memory mechanism can be explained by the hysteresis curves or by bistability (**Fig. 5.2B**). The change in  $y(2)$  and  $y(3)$  depended on the history of input signal  $S$ .  $y(2)$  and  $y(3)$  increased according to the dotted line in **Fig. 5.2B** with an increase in  $S$ , achieving a high level of gene expression, while  $y(2)$  and  $y(3)$  decreased along the solid curve with a decrease in  $S$ . Even after  $S$  decreased to zero, the protein levels were sustained at a high level, showing memory. Despite the difference in the dissociation constants, the deterministic memory was sustained (**Fig. 5.2A**). In contrast, the stochastic model represented the memory persistence at dissociation constants of  $K(2) = K(4) = 43$ , but it presented unsuccessful memory at dissociation constants of  $K(2) = K(4) = 46$  (**Fig. 5.2C and D**), where the levels of  $y(2)$  and  $y(3)$  returned to that before the signal input. Strong binding between activators and DNA strengthening a positive feedback loop was effective for memory persistence in a certain range. Noise or a stochastic perturbation flipped gene expression from one state to the other state

(Eldar and Elowitz, 2010), thus demonstrating that stochastic behavior deteriorates memory function.

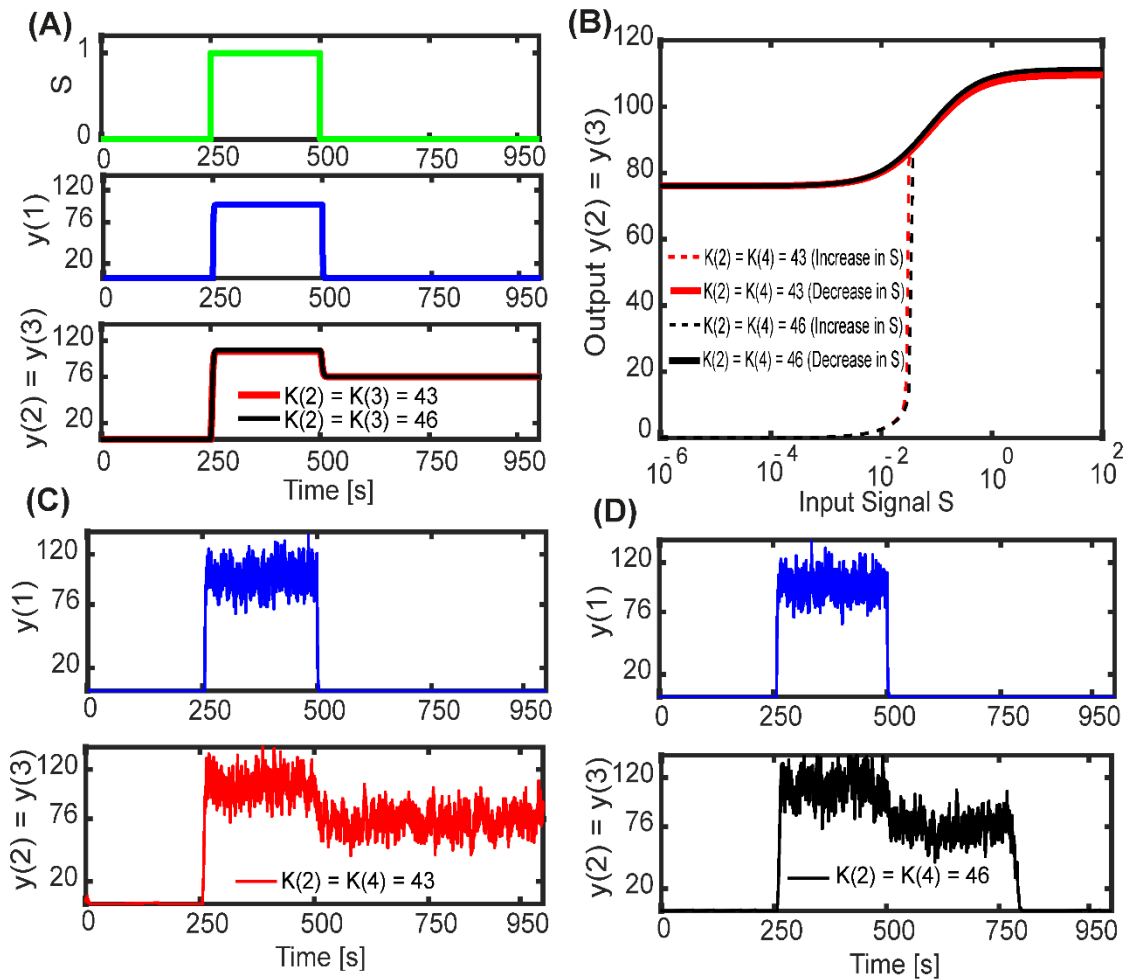


**Fig. 5.2 Deterministic and stochastic simulations of the MAN**

(A) Deterministic simulation of proteins  $y(1)$ ,  $y(2)$  and  $y(3)$ . Signal  $S$  is input from time 250 to 500. The red and black lines indicate  $y(2) = y(3)$  at dissociation constants  $K(2) = K(4) = 43$  and at  $K(2) = K(4) = 46$ , respectively. The Hill coefficient is set to  $n = 2$ . (B) Hysteresis curves of  $y(2) = y(3)$  at different dissociation constants. The red solid and dotted lines indicate  $y(2) = y(3)$  with respect to a decrease and an increase in  $S$  at  $K(2) = K(4) = 43$ , respectively. The black solid and dotted lines indicate  $y(2) = y(3)$

with respect to a decrease and an increase in  $S$  at  $K(2) = K(4) = 46$ , respectively. (C) Stochastic simulation of  $y(1)$ ,  $y(2)$  and  $y(3)$  at  $K(2) = K(4) = 43$ . (D) Stochastic simulation of  $y(1)$ ,  $y(2)$  and  $y(3)$  at  $K(2) = K(4) = 46$ .

### 5.3.2. MRN-generated memory function

We investigated the MRN at dissociation constant  $K(2) = K(4) = 43$  and the different Hill coefficients of  $n = 7$  and  $n = 8$ . The values of the corresponding kinetic parameters were set as shown in **Table 5.3**. The steady state levels of  $y(2)$  and  $y(3)$  were conserved as much as possible between the MRN and MAN (**Appendix A and B**). The high level of  $y(2)$  was set to be the same as that of  $y(2) = y(3)$  in the MAN. The dynamics of the MRN was simulated according to the Gillespie stochastic method. As shown in **Fig. 5.3A**, when a transient signal was input from time 250 to 500,  $S$ -induced  $y(1)$  activated  $y(2)$  and suppressed  $y(3)$ . The dynamic behavior of  $y(2)$  was opposed to that of  $y(3)$ , where it is impossible to set all the corresponding parameters between  $y(2)$  and  $y(3)$  within the model to the same values (**Appendix B**). Deterministic memory of the high and low levels of  $y(2)$  and  $y(3)$  was observed after 500, where a high level of  $y(2)$  and a low level of  $y(3)$  were maintained. The hysteresis behaviors of  $y(2)$  and  $y(3)$  were shown in the same manner as the MAN, as shown in **Fig. 5.3BC**.  $y(2)$  increased with an increase in  $S$ , but decreased in a different manner with a decrease in  $S$ ; in contrast,  $y(3)$  decreased with an increase in  $S$ , and increased in a different manner with a decrease in  $S$ . This hysteresis results from the bistability generated by mutual repression. Despite the difference in the Hill coefficient, the deterministic memory of  $y(2)$  and  $y(3)$  were sustained. On the other hand, the stochastic model represented the memory at  $n = 8$ , but provided unsuccessful memory at  $n = 7$  (**Fig. 5.3D E**):  $y(2)$  and  $y(3)$  returned to their

levels before the signal input. This finding demonstrated that stochastic behavior decreases memory function.

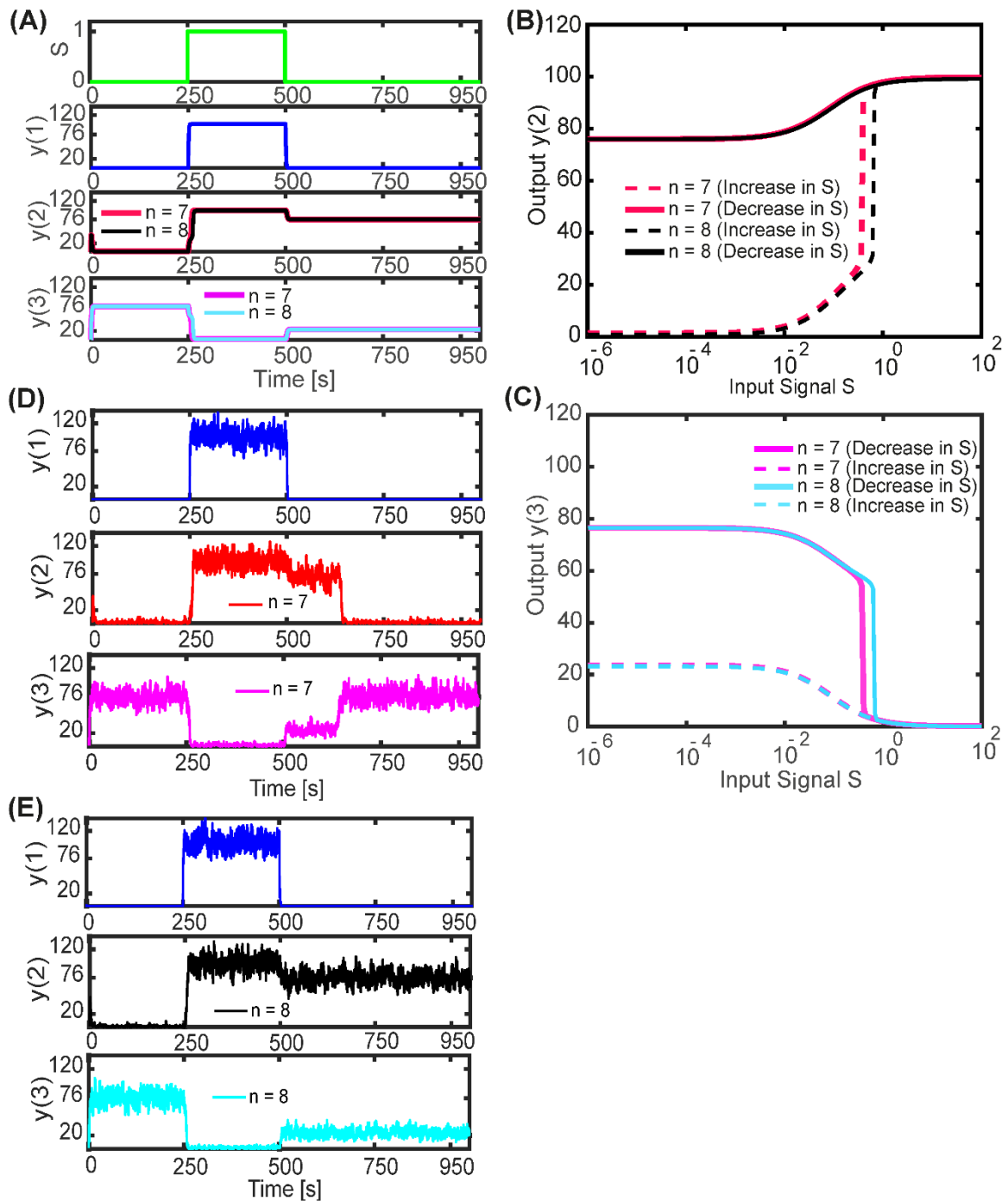


**Fig. 5.3 Deterministic and stochastic simulations of the MRN**

(A) Deterministic simulation of proteins  $y(1)$ ,  $y(2)$  and  $y(3)$ . Signal  $S$  is input from time 250 to 500. Dissociation constants are set to  $K(2) = K(4) = 43$  and other corresponding

parameter values are set the same as for the MAN. The red and magenta lines indicate  $y(2)$  and  $y(3)$  at  $n = 7$ , respectively. The black and cyan lines indicate  $y(2)$  and  $y(3)$  at  $n = 8$ , respectively. (B) Hysteresis curves of  $y(2)$  at different Hill coefficients. The red solid and dotted lines indicate  $y(2)$  with respect to a decrease and an increase in  $S$  at  $n = 7$ , respectively. The black solid and dotted lines indicate  $y(2)$  with respect to a decrease and an increase in  $S$  at  $n = 8$ , respectively. (C) Hysteresis curves of  $y(3)$  at different Hill coefficients. The magenta solid and dotted lines indicate  $y(3)$  with respect to a decrease and an increase in  $S$  at  $n = 7$ , respectively. The cyan solid and dotted lines indicate  $y(3)$  with respect to a decrease and an increase in  $S$  at  $n = 8$ , respectively. (D) Stochastic simulation of  $y(1)$ , and  $y(3)$  at Hill coefficient  $n = 7$ . (E) Stochastic simulation of  $y(1)$ ,  $y(2)$  and  $y(3)$  at Hill coefficient  $n = 8$ .

### 5.3.3. Simulation comparison between the MAN and MRN models

To analyze the mechanism by which different architectures of the MAN and MRN models alter the persistence of memory, we compared the memory functions while setting the values of the corresponding kinetic parameters within each model and between the competitive models to the same values and conserving the steady states levels of  $y(2)$  and  $y(3)$  as much as possible, as shown in **Table 5.2**. Details are described in **Appendix A-B**. We estimated the two-dimensional memory regions of the two models by conducting deterministic and stochastic simulations at each grid point as depicted in **Fig. 5.4**, where the x-axis and y-axis represent the Hill coefficient and dissociation constant, respectively. The kinetic parameter  $k(7)$  was adjusted so as to conserve the high steady-state level between the two models. The memory regions consist of two areas: (i) deterministic memory (green plus red areas in **Fig. 5.4**) and (ii)

stochastic persistent memory (red areas). The other areas indicate a monostable region or no memory region. The deterministic region was obtained by numerical simulations of Eqs. (5.1-5.6), and the stochastic persistent memory region was identified by our empirical rule defined in the Methods. The MAN generated both deterministic and stochastic memories at a Hill coefficient of  $n = 2$  (**Fig. 5.4A**). In contrast, the MRN required a Hill coefficient of  $n = 4$  to obtain deterministic memory and a coefficient of  $n = 8$  to achieve stochastic persistent memory. The stochastic persistent memory regions were included in the deterministic regions. The stochastic persistent memory region of the MAN was much larger than that of the MRN, indicating that the MAN readily presents a robust property of deterministic and stochastic persistent memory with respect to changes in the kinetic parameters. In the MRN, very high cooperativity was required to generate the stochastic persistent memory, and the stochastic persistent memory region was very limited and located close to the lower boundary of the dissociation constant.

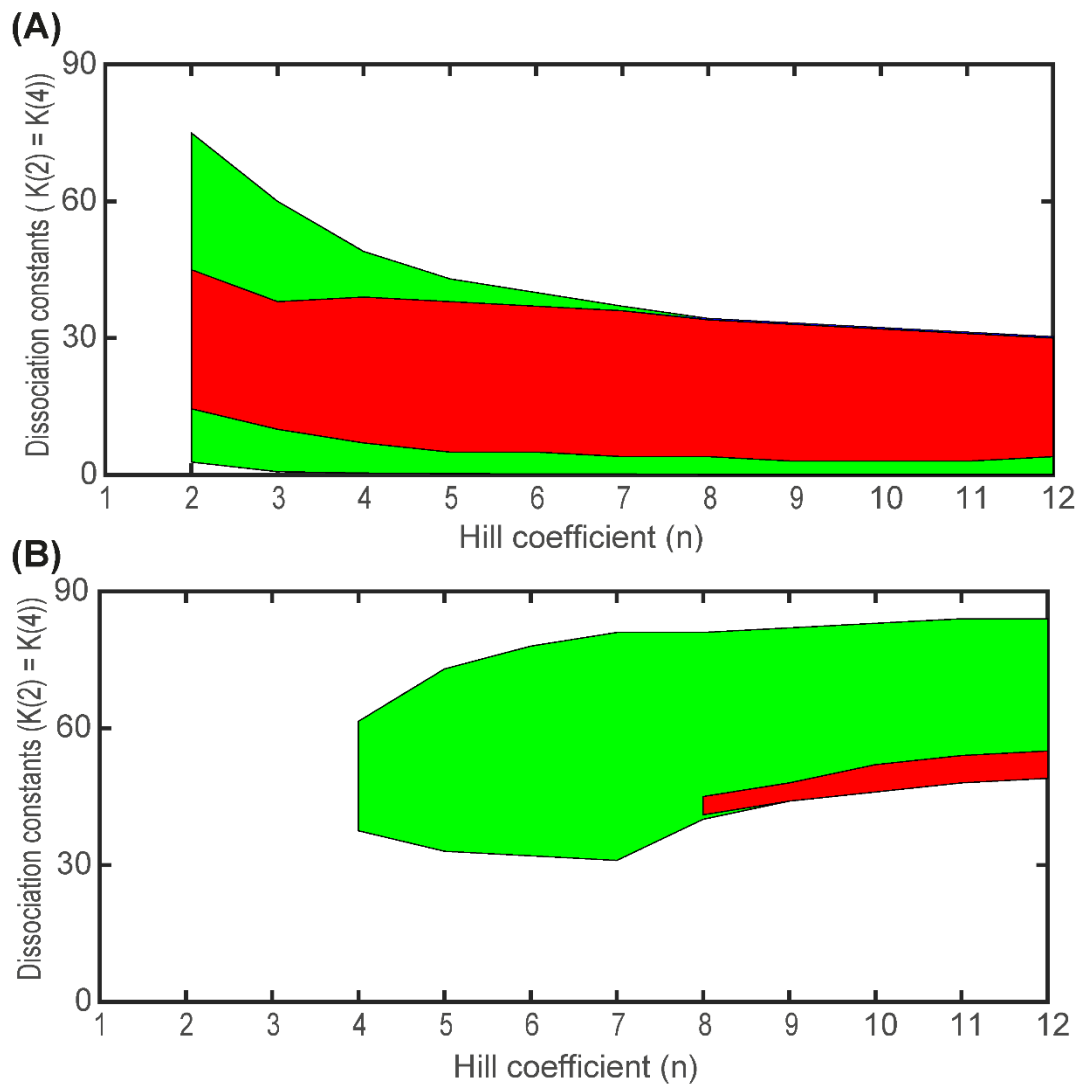


**Fig. 5.4 Comparisons of the memory regions among the two competitive models**

(A) Memory region of the MAN. (B) Memory region of the MRN. The memory regions are simulated with respect to the Hill coefficient and dissociation constants. The deterministic memory region is shown in green and red, whereas the stochastic memory regions are shown in red.

### 5.3.4. Comparison of the stochastic potential profile between the MAN and MRN models

Theoretical analysis with chemical master equations was performed to support the simulation results. The Fokker-Planck equations (Eq. (5.11)), which were derived by combining the three rate equations (Eqs. (5.1-5.3) and (5.4-5.6)), provided almost the same probability density as the Gillespie stochastic simulation (**Appendix E**). The theoretical analysis was confirmed to be consistent with the Gillespie stochastic simulation analysis. By using the Fokker-Planck equations, we estimated the two-dimensional stochastic bistable regions for the MAN and MRN models, where the x-axis and y-axis represent the Hill coefficient and dissociation constant, respectively, as depicted in **Fig. 5.5**. The stochastic bistable region was identified, as shown in **Appendix F**. The stochastic bistable regions of the MAN and MRN models are illustrated in red and blue, respectively, while changing the Hill coefficient and dissociation constant. The other corresponding kinetic parameters between the models were set to be the same (**Appendix A and B**). The MAN generated the bistable region at a Hill coefficient of  $n = 2$  (**Fig. 5.5A**), whereas the MRN required a Hill coefficient of  $n = 3$  to show bistability (**Fig. 5.5B and C**). The MRN required higher cooperativity than the MAN to generate stochastic bistability, indicating that the MAN more readily presents stochastic bistability than the MRN.

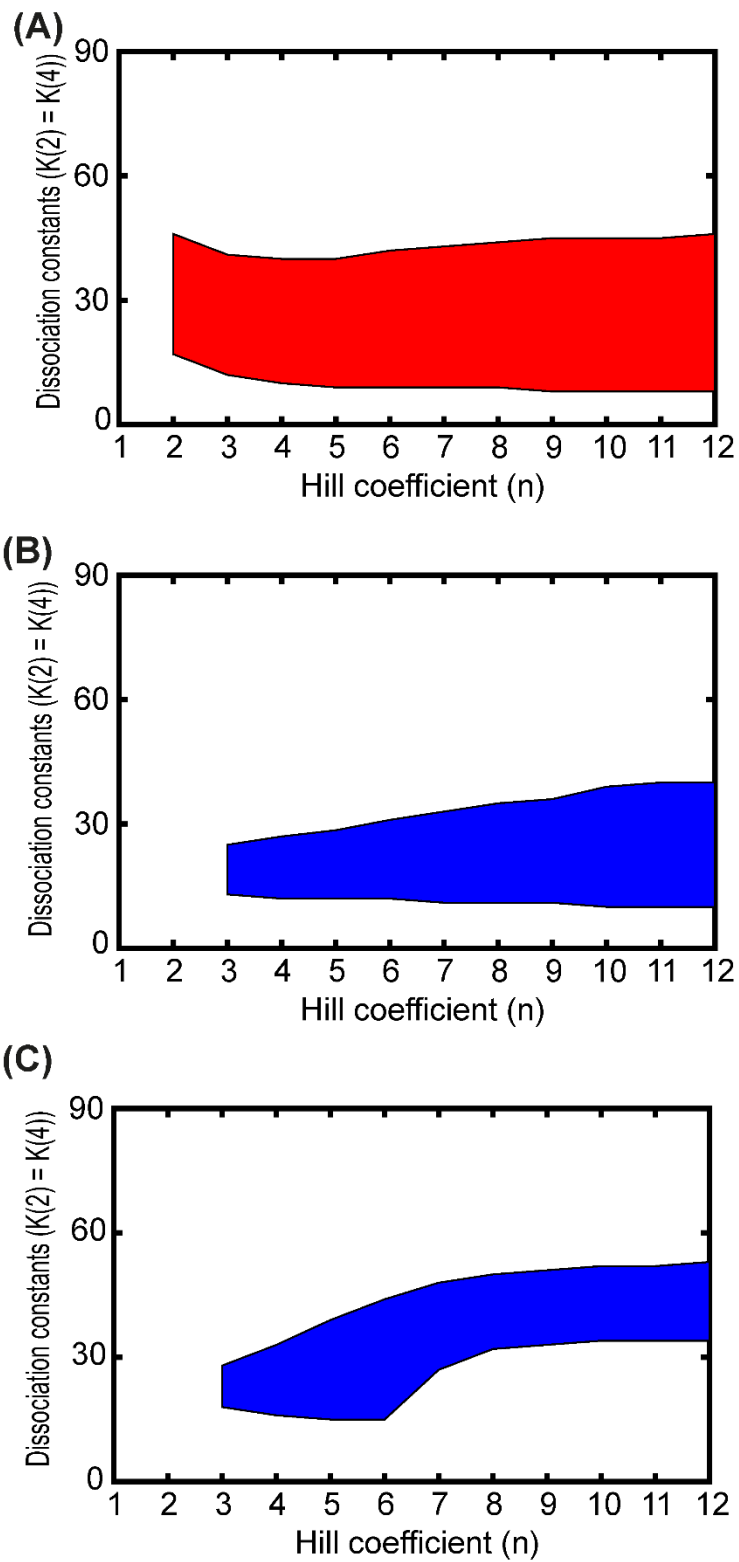


**Fig. 5.5 Comparisons of the stochastic bistable regions between the two competitive models**

(A) In the MAN, the stochastic bistable regions of  $y(2) = y(3)$  are shown with respect to the Hill coefficient and dissociation constant under noises.

(B-C) In the MRN, the stochastic bistable regions of  $y(2)$  (B) and  $y(3)$  (C) are shown with respect to the Hill coefficient and dissociation constant under noises.

### 5.3.5. Comparison of the MFPT between the MAN and MRN models

The stochastic bistable region indicates the bimodality of gene expression, but not the persistent memory. Thus, the MFPT was employed to characterize the stochastic persistent memory or to support the simulation result that the stochastic persistent memory region is very small in the MRN model. As shown in **Fig. 5.6**, the logarithmic MFPTs of  $y(2)$  and  $y(3)$  were calculated for the MAN and MRN models. The low and high steady-states of  $y(2)$  and  $y(3)$  are denoted as  $y(2)_l^{st}$ ,  $y(2)_u^{st}$ ,  $y(3)_l^{st}$  and  $y(3)_u^{st}$ , respectively. In the MAN,  $T_L(y(2)_l^{st})$  and  $T_U(y(2)_u^{st})$  were identical to  $T_L(y(3)_l^{st})$  and  $T_U(y(3)_u^{st})$  because their corresponding kinetic parameters between  $y(2)$  and  $y(3)$  were set to be the same. The effect of the Hill coefficient or cooperativity on the MFPTs of  $y(2)$  and  $y(3)$  was investigated. For both the models, an increase in the Hill coefficient lengthened the MFPTs, sustaining stochastic memory. In the MAN  $T_U(y(2)_u^{st})$  was much longer than  $T_L(y(2)_l^{st})$ , indicating that the high expression level of  $y(2) = y(3)$  is more persistent.  $T_L(y(2)_l^{st})$  and  $T_U(y(2)_u^{st})$  of the MAN were longer than  $T_L(y(2)_l^{st})$ ,  $T_U(y(2)_u^{st})$ ,  $T_L(y(3)_l^{st})$  and  $T_U(y(3)_u^{st})$  of the MRN with respect to a Hill coefficient, indicating that the MAN shows more persistent memory than the MRN. To lengthen the MFPT of the MRN, it is required to increase the Hill coefficient.

The effect of the dissociation constants on the MFPTs of  $y(2)$  and  $y(3)$  was investigated.  $T_L(y(2)_l^{st})$  and  $T_U(y(2)_u^{st})$  of the MAN were longer than  $T_L(y(2)_l^{st})$ ,  $T_L(y(3)_l^{st})$ ,  $T_U(y(2)_u^{st})$  and  $T_U(y(3)_u^{st})$  of the MRN for all the dissociation constants. It indicates that the MAN generated more persistent memory than the MRN. In other words, the MRN memory is fragile. In the MAN, an increase in the dissociation constant increased  $T_L(y(2)_l^{st})$ , but decreased  $T_U(y(2)_u^{st})$ , indicating that strong binding of the activator results in a persistent high expression level. The results also suggest that gene expression transitions from a high-steady state to a low-steady state with an increase in the dissociation constant. In the MRN,  $T_L(y(2)_l^{st})$ ,  $T_U(y(2)_u^{st})$ ,  $T_L(y(3)_l^{st})$  and  $T_U(y(3)_u^{st})$  gradually decreased with an increase in the dissociation constant, indicating that strong binding repressors are necessary for persistent memory.

To illustrate changes in the stochastic gene expression profile, we calculated the probability density (Eq. (5.18)) for the MAN and MRN models with respect to the Hill coefficient and dissociation constants, as shown in **Fig. 5.7**. In the MAN, as shown in **Fig. 5.7A**, a change in the Hill coefficient ( $n \geq 2$ ) hardly affected the probability density of a high-steady-state level of  $y(2)=y(3)$  in the MAN. Low cooperativity was sufficient to make a high-steady-state level dominant. In the MRN, as shown in **Fig. 5.7B**, an increase in the Hill coefficient increased the probability density of a high-steady-state level, decreasing that of a low-steady-state level, which made a high-steady-state level of  $y(2)$  dominant. In **Fig. 5.7C**, an increase in the Hill coefficient decreased the probability density of a low-steady state level, but it also decreased that between the high- and low-steady-state levels, which clearly separated the low-steady state level from the high-steady-state level. This would contribute to enhanced sustainability of a low-steady-state level of  $y(3)$ . In the MAN, as shown in **Fig. 5.7D**, a decrease in the dissociation

constant (strong binding) slightly increased the probability density of a high-steady-state level of  $y(2)=y(3)$  and decreased that of a low-steady state level, which made a high-steady-state dominant. In the MRN, as shown in **Fig. 5.7E**, a decrease in the dissociation constant enhanced the probability density of a high-steady-state level, decreasing that of a low-steady-state level, which made a high-steady-state of  $y(2)$  dominant. In **Fig. 5.7F**, a decrease in the dissociation constant decreased the probability density of a low-steady state level, but also decreased that between the high- and low-steady-state levels, which clearly separated the low-steady state level from the high-steady-state level. This would contribute to enhanced sustainability of a low-steady-state level of  $y(3)$ .

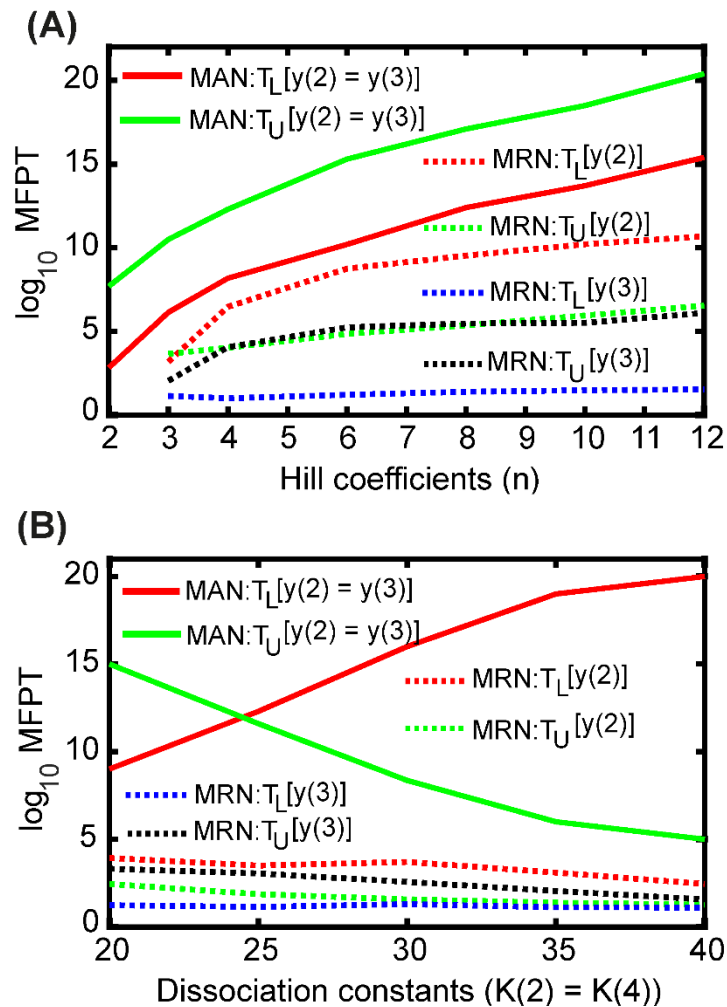


**Fig. 5.6** Comparisons of the MFPTs between the two competitive models

(A) The logarithmic MFPTs of  $y(2)$  and  $y(3)$  were compared between the MAN and MRN models with respect to the Hill coefficient under noises. The dissociation constants are set to  $K(2) = K(4) = 15$  in the MAN. The dissociation constants are  $K(2) = K(4) = 15$  and  $K(2) = K(4) = 35$  for  $y(2)$  and  $y(3)$ , respectively, in the MRN.

(B) The logarithmic MFPTs of  $y(2)$  and  $y(3)$  were compared between the MAN and MRN with respect to the dissociation constant under noises. The Hill coefficient was set to  $n = 3$  in both models.

The red and green solid lines indicate  $T_L(y(2)_l^{st}) = T_U(y(3)_u^{st})$  and  $T_U(y(2)_u^{st}) = T_L(y(3)_l^{st})$  for the MAN, respectively. The red and green dotted lines indicate  $MFPT_L(y(2)_l^{st})$  and  $MFPT_U(y(2)_u^{st})$  for the MRN, respectively. The blue and black dotted lines indicate  $T_U(y(3)_u^{st})$  and  $T_L(y(3)_l^{st})$  for the MRN, respectively.

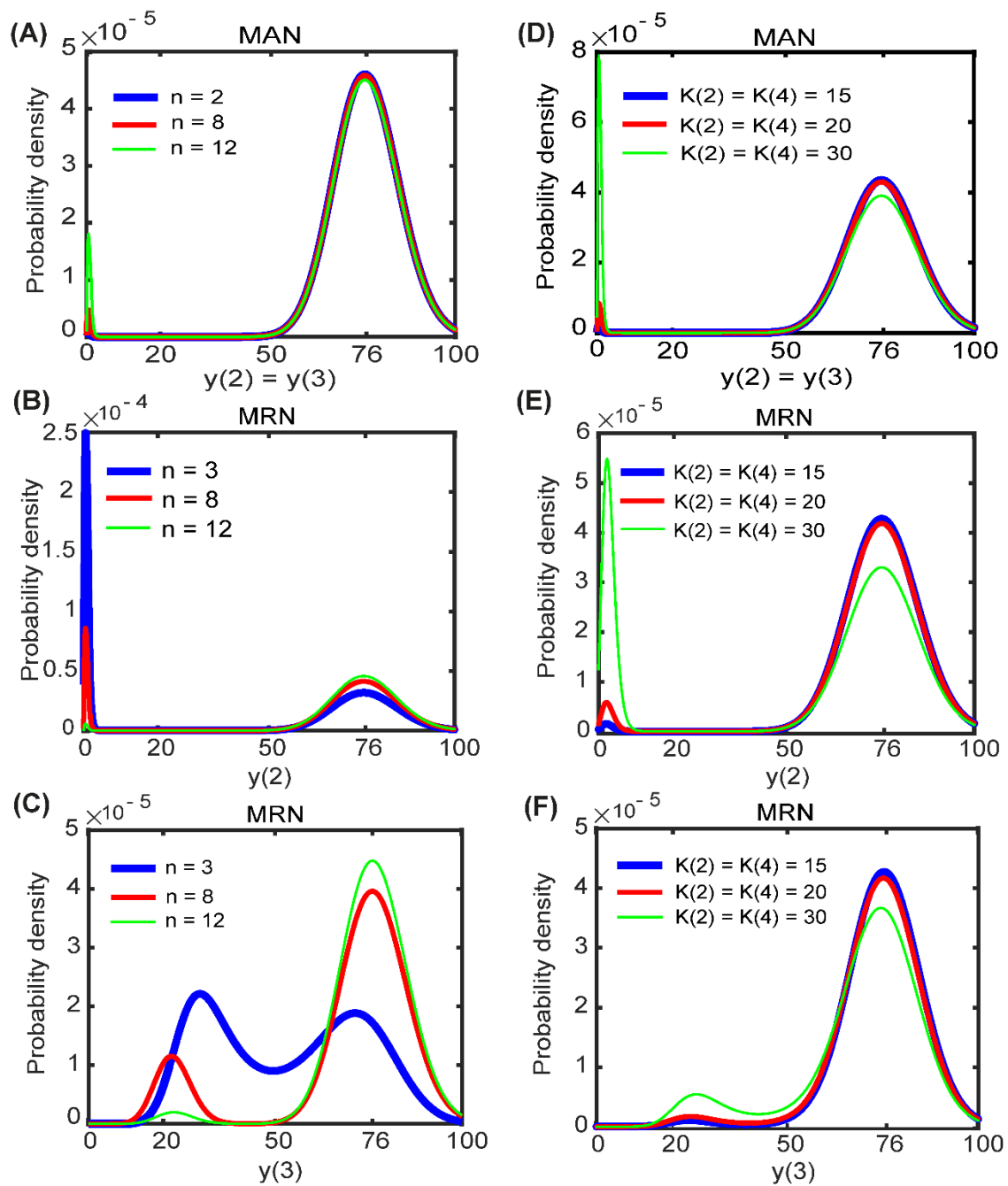


**Fig. 5.7 Comparison of the probability density of the steady-state level between the two competitive models**

(A) Probability density of  $y(2) = y(3)$  of the MAN with respect to the Hill coefficient. (B) Probability density of  $y(2)$  of the MRN with respect to the Hill coefficient. (C) Probability density of  $y(3)$  of the MRN with respect to the Hill coefficient. (A-C) The blue, red and green

lines indicate  $n = 2$ , ( $n = 3$  for MRN)  $n = 8$  and  $n = 12$ , respectively. The dissociation constant was set to  $K(2) = K(4) = 15$  in both models.

(D) Probability density of  $y(2) = y(3)$  of the MAN with respect to the dissociation constant.

(E) Probability density of  $y(2)$  of the MRN with respect to the dissociation constant. (F)

Probability density of  $y(3)$  of the MRN with respect to the dissociation constant. (D-F) The

blue, red and green lines indicate  $K(2) = K(4) = 15$ ,  $K(2) = K(4) = 20$  and

$K(2) = K(4) = 30$ , respectively. The Hill coefficient was set to  $n = 3$  in both models. (A-

F) Fokker-Planck equations are used.

## 5.4. Discussion

We focused on revealing the requirement of the persistence or sustainability of a gene expression level in response to transient signals. So far the MAN and MRN have been analyzed separately and their differences in memory were not identified in silico and in vivo. To our limited knowledge, this is the first report that reveals mechanisms by which the structural differences between the MAN and MRN alter memory persistence. We analyzed the mechanisms by which mutual activation and repression networks generate a robust, persistent memory in the presence of noise. Stochasticity decreased the memory persistence of both models. In particular, the stochastic memory of the MRN was very fragile in the presence of noise. In contrast, the MAN achieved robust, persistent memory in both the deterministic and stochastic approaches at a lower cooperativity than the MRN. The stochastic memory pattern of the MAN can be adjusted by changing the binding strength of the activators (**Fig. 5.6B**). The MRN required highly cooperative and strong binding repressors for robust memory.

Mathematical comparison allowed characterization of the memory region between the competitive networks. We set the corresponding kinetic parameters within each model and between the MAN and MRN models to be as same as possible and also conserved the high steady-state levels between the models. Two-dimensional memory analysis with respect to the Hill coefficient and dissociation constant was effective in characterizing the memory function and bimodality, and these two kinetic parameters were responsible for the cooperativity and binding strength of the activators or repressors. The Gillespie algorithm accurately simulated the time-course of changes in protein concentration but had difficulty in rigorously identifying the stochastic persistent memory region due to the complexity of the calculation. Many time-consuming simulations are required to determine if the model shows stochastic persistent memory, whereas theoretical analysis overcomes this calculation complexity. The stochastic potential profile accurately illustrated if the model shows bistability, but did not indicate the persistence of memory. Thus, the MFPT was used to characterize memory sustainability. A high value of the MFPT means that the level is memorized or sustained for a long period of time, whereas a low value indicates that the level quickly transitions to another level.

The MFPT analysis indicated that the stochastic persistent memory achieved by the MAN was more robust and persistent than that achieved by the MRN, because the MFPTs of the low and high steady-states of  $y(2)$  and  $y(3)$  in the MAN were much longer than those of the MRN. This supported the simulation result that the stochastic persistent memory region of the MRN is very limited. In addition, the present findings revealed the mechanism by which the cooperativity and binding strength of the activators or repressors affect the stochastic persistent memory of the MAN and MRN. For both models, high cooperativity prolonged the MFPT, sustaining the memory function. On the other hand, a decrease in the dissociation constant (or an increase in

the binding strength) decreased  $T_L(y(2)_l^{st})$ , but increased  $T_U(y(2)_u^{st})$  in the MAN. A high steady-state level was memorized or sustained at a low dissociation constant, whereas a low steady-state level was sustained at a high dissociation constant. It indicates that the memory pattern of the MAN can be controlled by changes in the dissociation constant. In the MRN, a decrease in the dissociation constant gradually increased the MFPTs. The MRN required strong binding repressors for sustained memory, which is consistent with the stochastic persistent memory of the MRN being located close to the lower boundary of the dissociation constant. Since the MFPT gradually changes with respect to a change in the dissociation constant, the memory pattern of the MRN would be hard to be controlled by changes in the binding strength of the repressor. To our limited kinetic conditions, since the MFPTs of the MRN were much shorter than those of the MAN, the MRN would be hard to become as robust as the MAN.

In this analysis, we used a specific set of the kinetic parameters and did not intensively investigate the dependency of stochastic memory on kinetic parameter values. Instead of it, we searched two-dimensional parameter region to make mathematical comparison reliable. In general, stochastic behaviors depend on the number of molecules within a cell. A large number of molecules can decrease stochastic effects, while a small number of molecules are very susceptible to stochasticity, which may cause unexpected dynamics. In this study, we used a middle number of repressors and activators and identified the structural difference greatly alters memory persistence. In next, we will investigate how a small number of molecules within a cell affect the stochastic persistent memory while changing the values of kinetic parameters. In addition, although the employed theoretical and simulation analyses were suited for the plain networks, it will be required to analyze complex models. For example, it would be interesting

to design a complex mutual repression module that achieves persistent memory. In this case, high-speed algorithms such as the tau-leap method (Cao et al., 2006) would be necessary.

For theoretical analysis, we reduced the three-variable equations to the one-variable equation. On the other hand, it is suggested the model reduced by the quasi-steady-state approximation is not always consistent with the full, origin model (Thomas et al., 2011), although the quasi-steady-state approximation is widely used. In next we investigate how relative errors between the reduced and full models are produced to confirm the results.

The MAN provided a robust memory region or sustained gene expression where the dynamic behaviors of two proteins were the same, whereas the MRN provided the opposite gene expression and fragile memory. This mathematical comparison provides guidance on whether we should select the MAN or MRN for an optimal, rational design. If a robust memory is required, a mutual activation network should be selected. If the opposite state of protein synthesis is necessary, a mutual repression network must be selected, although the memory effect is fragile (Gardner et al., 2000). This fragility may be related to the fact that suppression cascades amplify noise compared with activation cascades (Acar et al., 2005). A mutual activation network comprising two protein kinases, p42 MAPK and Cdc2, is suggested to require robust memory (Xiong and Ferrell, 2003; Huang and Ferrell, 1996). The MAN seems to evolve in the context of signaling networks to make memory within a cell or to irreversibly change its gene expression level. On the other hand, a mutual repression network comprising the cI and Cro proteins would require a gene expression system opposite to that of robust memory (Casadesus and D'Ari, 2002). A Notch-Delta mutual repression network is an intelligible example to communicate between neighboring cells (Matsuda et al., 2015). An increase in Notch activity within a cell decreases Notch activity in neighboring cells, and thus

Notch-Delta mutual repression provides inhomogeneous or opposite protein synthesis in homogeneous cell populations. Generally, differentiation requires spatial changes in gene expression. The MRN takes advantage of opposite gene expression between neighboring cells at different steps during cell lineage progression, thus contributing to differentiation decisions or signaling diversity not only across a wide spectrum of species but also across a broad range of cell types in a single organism. To differentiate cells with different functions, the MRN may evolve despite its fragile memory. To overcome the fragility of the MRN, complex networks would be necessary. For example, the addition of negative feedback loops to the MRN can stabilize the gene expression level or enhance memory function, although few studies pointed out it.

# CHAPTER 6

## Conclusion and Future Works

### 6.1 Conclusion

We focused on the quantitative understanding of the dynamical behavior in the gene expression due to mathematical modeling. During our research, we have built up various kind of genetic networks to reveal the mechanism of noise in gene expression at the steady-state level such as open-loop system ACN and RCN models, closed-loop system ACN and RCN models through the strong-weak dissociation constants. As for example, in RCN model apparently increased the noise at strong dissociation constant which is opposite to ACN model. Because the mechanisms of genetic noise are one of the ubiquitous problems in the system as well as quantitative biology. Also, we reported two-gene tMAN and tMRN models, to use non-symmetric kinetics parameters set for a range of biologically relevant conditions thus shown stochastic bimodality, even multimodality exist in deterministically monostable regime while non-cooperative binding. Therefore, bimodality, multimodality are observed not only for parameter values corresponding to deterministic but also beyond it occurred as the discreteness amplification of the molecular concentration of proteins.

We employed the mathematical comparison which was used to analyze the deterministic or stochastic memory functions between the proposed competitive models at the same steady state level. The MAN model improved the memory function in both deterministic and stochastic models, compared with the MRN model. The MAN provided a robust memory window and consistent gene expression, where the synthesis levels of two proteins were always the same. On the other hand, the MRN provided opposite gene expressions with a fragile memory. The MAN model that comprises two protein kinases p42 MAPK and Cdc2 are suggested to need

robust memory. On the other hand, the MRN model that consists of cI and Cro proteins would require opposite gene expression rather than robust memory. Also, a Notch-Delta mutual repression network is an intelligible example to communicate between neighboring cells. The mathematical comparison to the achievement of the biological memory of the theoretical networks improved an understanding of the potential applications of engineered memory networks in medicine and industrial biotechnology.

## 6.2 Extended to future works

In the MRN, we added negative autoregulations to  $y(2)$  and  $y(3)$  syntheses to investigate how negative feedback loops affect their memory functions, as shown in Fig. 6.1. This model is named the regulated mutual repression network model with negative autoregulations (MRN-NA).

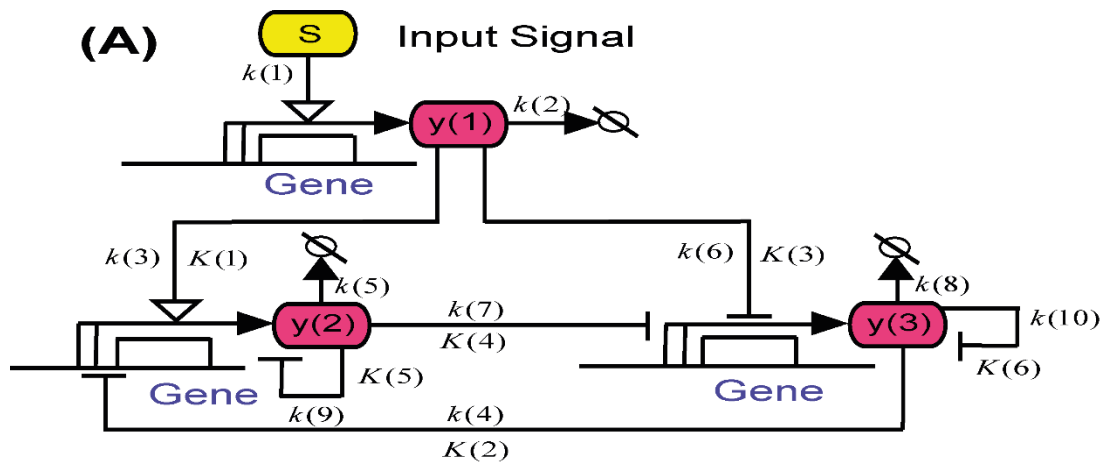


**Fig. 6.1 MRN-NA. Negative autoregulations are added to the MRN model.**

Also, we will be constructed, regulated the combined activation coupled oscillators (ACO), regulated the combined of repression coupled oscillators (RCO) models as shown in Fig. 6.2. We will be able to show the novel design mechanism of robust oscillatory function in noise-induced gene expression.

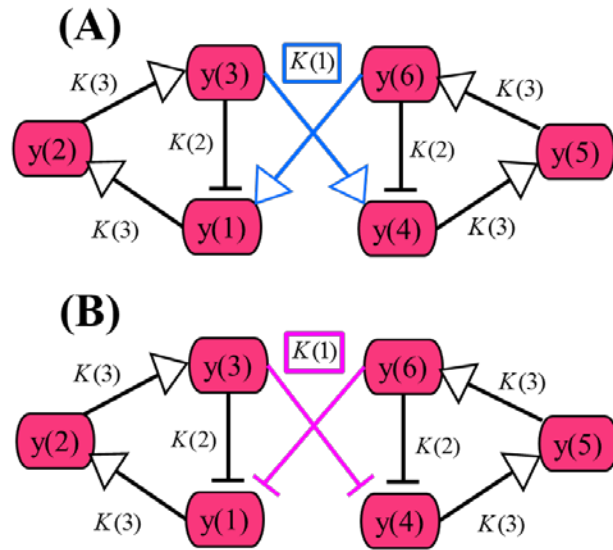


**Fig 6.2. Two competitive oscillator network maps**

(A) ACO. Protein  $y(3)$  and  $y(6)$  acts as mutual activation network consisting of the two repressilator networks of proteins of  $y(1)$ ,  $y(2)$ ,  $y(4)$  and  $y(5)$ . (B) RCO. Protein  $y(3)$  and  $y(6)$  acts as mutual repression network consisting of the two repressilator networks of proteins of  $y(1)$ ,  $y(2)$ ,  $y(4)$  and  $y(5)$ .

## Appendix A. Parameter settings of the MAN

The MAN is given by Eqs. (5.1-5.3). When the corresponding parameters between Eqs. (5.2, 5.3) are set to be the same as follows:

$$k(3) = k(6), \quad k(4) = k(7), \quad k(5) = k(8), \quad K(1) = K(3), \quad K(2) = K(4),$$

the steady-state solution is given by:

$$y_{ss}(1) = \frac{k(1) \cdot S}{k(2)} \quad (\text{A1})$$

$$y_{ss}(2) = \left\{ b + k(3) \cdot \frac{y_{ss}(1)}{y_{ss}(1) + K(1)} + k(4) \cdot \frac{y_{ss}(3)^n}{y_{ss}(3)^n + K(2)^n} \right\} \cdot \frac{1}{k(5)} \quad (\text{A2})$$

$$y_{ss}(3) = \left\{ b + k(3) \cdot \frac{y_{ss}(1)}{y_{ss}(1) + K(1)} + k(4) \cdot \frac{y_{ss}(2)^n}{y_{ss}(2)^n + K(2)^n} \right\} \cdot \frac{1}{k(5)} \quad (\text{A3}),$$

where

$$k(4) = k(7) = \left\{ k(5) \cdot y_{ss}(2) - b - k(3) \cdot \frac{y_{ss}(1)}{y_{ss}(1) + K(1)} \right\} \cdot \frac{y_{ss}(3)^n + K(2)^n}{y_{ss}(3)^n} \quad (\text{A4}).$$

Subscript *ss* indicates the steady state. Values of  $k(4) = k(7)$  are determined so that the high and low steady-state levels of  $y_{ss}(2) = y_{ss}(3)$ , respectively, can be set to specific levels.

## Appendix B. Parameter settings of the MRN

The MRN model is given by Eqs. (5.4-5.6). When the corresponding parameters between Eqs. (5.5, 5.6) are set to be the same as follows:

$$k(3) = k(6), \quad k(5) = k(8), \quad K(1) = K(3), \quad K(2) = K(4),$$

the steady state solution is given by:

$$y_{ss}(1) = \frac{k(1) \cdot S}{k(2)} \tag{B1}$$

$$y_{ss}(2) = \left\{ k(3) \cdot \frac{y_{ss}(1)}{y_{ss}(1) + K(1)} + k(4) \cdot \frac{K(2)^n}{y_{ss}(3)^n + K(2)^n} \right\} \cdot \frac{1}{k(5)} \tag{B2}$$

$$y_{ss}(3) = \left\{ k(3) \cdot \frac{K(1)}{y_{ss}(1) + K(1)} + k(7) \cdot \frac{K(2)^n}{y_{ss}(2)^n + K(2)^n} \right\} \cdot \frac{1}{k(5)} \tag{B3},$$

where

$$k(4) = \left\{ k(5) \cdot y_{ss}(2) - k(3) \cdot \frac{y_{ss}(1)}{y_{ss}(1) + K(1)} \right\} \cdot \frac{y_{ss}(3)^n + K(2)^n}{K(2)^n} \tag{B4}$$

$$k(7) = \left\{ k(5) \cdot y_{ss}(3) - k(3) \cdot \frac{K(1)}{y_{ss}(1) + K(1)} \right\} \cdot \frac{y_{ss}(2)^n + K(2)^n}{K(2)^n} \tag{B5}.$$

The value of  $k(7)$  is fixed and the value of  $k(4)$  ( $> k(7)$ ) is determined so that the high steady-states of  $y_{ss}(2)$  and  $y_{ss}(3)$  can be set to a specific level. The levels of  $y_{ss}(2)$  and  $y_{ss}(3)$  are

always opposite due to mutual repression. When the high steady-state levels are the same, it is very difficult to conserve the low steady-states of  $y_{ss}(2)$  and  $y_{ss}(3)$  at the same level.

## Appendix C. One-variable equation and noise function of the MAN

To perform deterministic and stochastic potential analysis, we converted the reaction rate equations (Eqs. (5.1-5.3)) into a one-variable rate equation. By setting  $S = 0$ , the MAN model is simplified into:

$$\frac{dy(2)}{dt} = b + k(4) \cdot \frac{y(3)^n}{y(3)^n + K(2)^n} - k(5) \cdot y(2) \quad (C1)$$

$$\frac{dy(3)}{dt} = b + k(7) \cdot \frac{y(2)^n}{y(2)^n + K(4)^n} - k(8) \cdot y(3) \quad (C2).$$

By applying the quasi-steady-state approximation to  $y(3)$ , the rate equation of  $y(2)$  is given by:

$$f_{MAN2}(y(2)) = b + k(4) \cdot \frac{y_{ss}(3)^n}{y_{ss}(3)^n + K(2)^n} - k(5) \cdot y(2) \quad (C3),$$

$$\text{where } y_{ss}(3) = \left\{ b + k(7) \cdot \frac{y(2)^n}{y(2)^n + K(4)^n} \right\} \cdot \frac{1}{k(8)} \quad (C4).$$

Consequently the rate equation is given by:

$$f_{MAN2}(y(2)) = b + k(4) \cdot \frac{\left[ \left\{ b + k(7) \cdot \frac{y(2)^n}{y(2)^n + K(4)^n} \right\} \cdot \frac{1}{k(8)} \right]^n}{\left[ \left\{ b + k(7) \cdot \frac{y(2)^n}{y(2)^n + K(4)^n} \right\} \cdot \frac{1}{k(8)} \right]^n + K(2)^n} - k(5) \cdot y(2) \quad (C5)$$

The noise function is given by (Cheng et al., 2008, Scott et al., 2007):

$$g_{MAN2}(y(2)) = b + k(4) \cdot \frac{[b + k(7) \cdot \frac{y(2)^n}{y(2)^n + K(2)^n}] \cdot \frac{1}{k(8)}]^n}{[\{b + k(7) \cdot \frac{y(2)^n}{y(2)^n + K(2)^n}\} \cdot \frac{1}{k(8)}]^n + K(2)^n} + k(5) \cdot y(2) \quad (C6)$$

In the same manner, the rate equation of  $y(3)$  is given by:

$$f_{MAN3}(y(3)) = b + k(7) \cdot \frac{[\{b + k(4) \cdot \frac{y(3)^n}{y(3)^n + K(2)^n}\} \cdot \frac{1}{k(5)}]^n}{[\{b + k(4) \cdot \frac{y(3)^n}{y(3)^n + K(2)^n}\} \cdot \frac{1}{k(5)}]^n + K(4)^n} - k(8) \cdot y(3) \quad (C7),$$

and the noise function is given by (Cheng et al., 2008, Scott et al., 2007):

$$g_{MAN3}(y(3)) = b + k(7) \cdot \frac{[\{b + k(4) \cdot \frac{y(3)^n}{y(3)^n + K(2)^n}\} \cdot \frac{1}{k(5)}]^n}{[\{b + k(4) \cdot \frac{y(3)^n}{y(3)^n + K(2)^n}\} \cdot \frac{1}{k(5)}]^n + K(4)^n} + k(8) \cdot y(3) \quad (C8).$$

## Appendix D. One-variable equation and noise function of the MRN

By setting  $S = 0$ , the MRN model (Eqs. (5.4-5.6)) is simplified into:

$$\frac{dy(2)}{dt} = k(4) \cdot \frac{K(2)^n}{y(3)^n + K(2)^n} - k(5) \cdot y(2) \quad (D1)$$

$$\frac{dy(3)}{dt} = k(6) + k(7) \cdot \frac{K(4)^n}{y(2)^n + K(4)^n} - k(8) \cdot y(3) \quad (D2).$$

By applying the quasi-steady-state approximation to  $y(3)$ , the one-variable rate equation of  $y(2)$  is given by:

$$f_{MRN2}(y(2)) = k(4) \cdot \frac{K(2)^n}{y_{ss}(3)^n + K(2)^n} - k(5) \cdot y(2) \quad (D3),$$

where 
$$y_{ss}(3) = \left\{ k(6) + k(7) \cdot \frac{K(2)^n}{y(2)^n + K(2)^n} \right\} \cdot \frac{1}{k(8)} \quad (D4).$$

Consequently, the rate equation is given by:

$$f_{MRN2}(y(2)) = k(4) \cdot \frac{K(2)^n}{\left[ \left\{ k(6) \cdot \frac{K(2)^n}{y(2)^n + K(2)^n} \right\} \cdot \frac{1}{k(8)} \right]^n + K(2)^n} - k(5) \cdot y(2) \quad (D5),$$

and the noise function is expressed as (Cheng et al., 2008, Scott et al., 2007):

$$g_{MRN2}(y(2)) = k(4) \cdot \frac{K(2)^n}{\left[ \left\{ k(6) \cdot \frac{K(2)^n}{y(2)^n + K(2)^n} \right\} \cdot \frac{1}{k(8)} \right]^n + K(2)^n} + k(5) \cdot y(2) \quad (D6),$$

In the same manner, the rate equation of  $y(3)$  is given by:

$$f_{MRN3}(y(3)) = k(6) + k(7) \cdot \frac{K(4)^n}{[k(4) \cdot \frac{K(2)^n}{y(3)^n + K(2)^n} \cdot \frac{1}{k(5)}]^n + K(4)^n} - k(8) \cdot y(3) \quad (D7),$$

and the noise function is given by (Cheng et al., 2008, Scott et al., 2007):

$$g_{MRN3}(y(3)) = k(6) + k(7) \cdot \frac{K(4)^n}{[k(4) \cdot \frac{K(2)^n}{y(3)^n + K(2)^n} \cdot \frac{1}{k(5)}]^n + K(4)^n} + k(8) \cdot y(3) \quad (D8).$$

## Appendix E. Consistency between the Gillespie stochastic simulation and the Fokker-Planck equation

The Fokker-Planck equations provided almost the same probability density as the Gillespie stochastic simulation (**Fig. E1**).

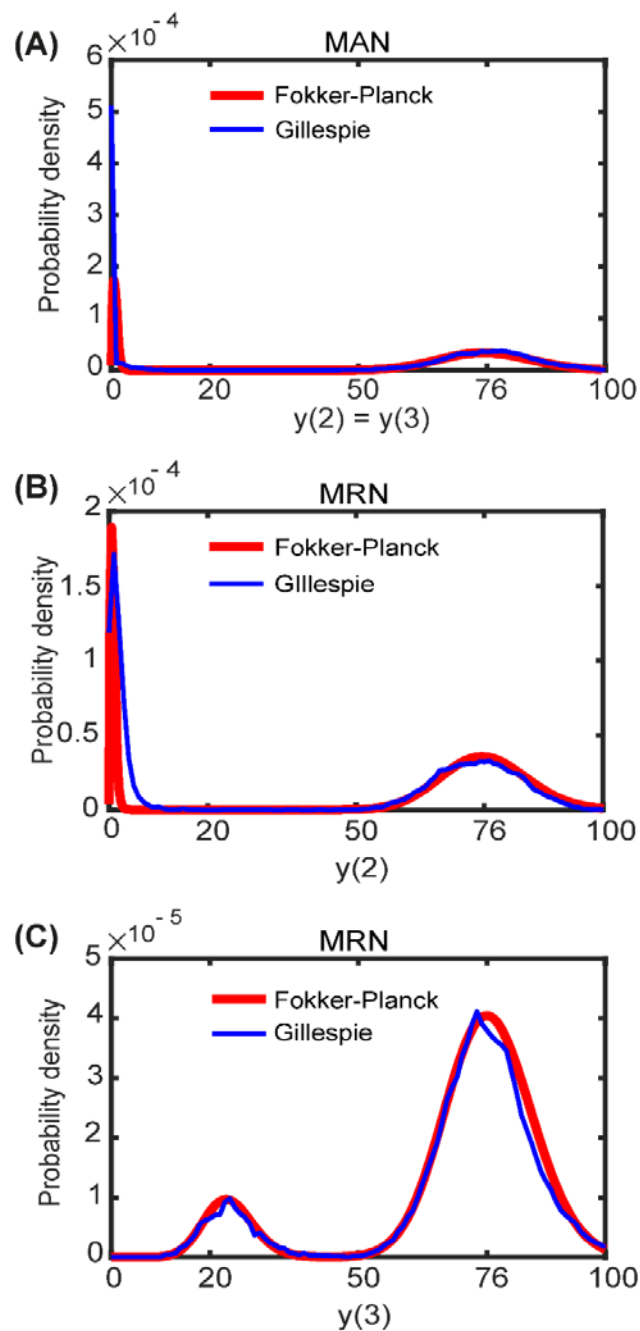


**Fig. E1** Probability density of the MAN and MRN models

(A) Probability density of  $y(2) = y(3)$  in the MAN model. The parameters are given as  $S = 0$ ,  $K(1) = K(3) = 9$ ,  $K(2) = K(4) = 34$ ,  $k(3) = k(6) = 18.1$ ,  $k(4) = k(7) = 72.95$ ,  $k(5) = k(8) = 0.8$ ,  $b = 0.01$ ,  $n = 2$ .

(B, C) Probability density of  $y(2)$  (B) and of  $y(3)$  (C) in the MRN model. The parameters are given as  $S = 0$ ,  $K(1) = K(3) = 9$ ,  $K(2) = K(4) = 43$ ,  $k(3) = k(6) = 18.1$ ,  $k(4) = 61.23 >$   
 $k(7) = 43.1$ ,  $k(5) = k(8) = 0.8$ ,  $n = 8$ .

## Appendix F. Stochastic potential analysis

We estimated the stochastic potential profile of the one-variable rate equation deriving from the MAN and MRN models (**Fig. F1**). In the stochastic potential profile, the two local minimums, corresponding to the low and high steady-state levels of  $y(2)$  and  $y(3)$ , indicated stable equilibrium points separated by the energy potential barrier at the local maximum or unstable equilibrium point. Stochastic bistability was identified by the existence of two local minimums. A system can transition from one state of minimal potential to the other if it is perturbed to overcome the potential barrier.

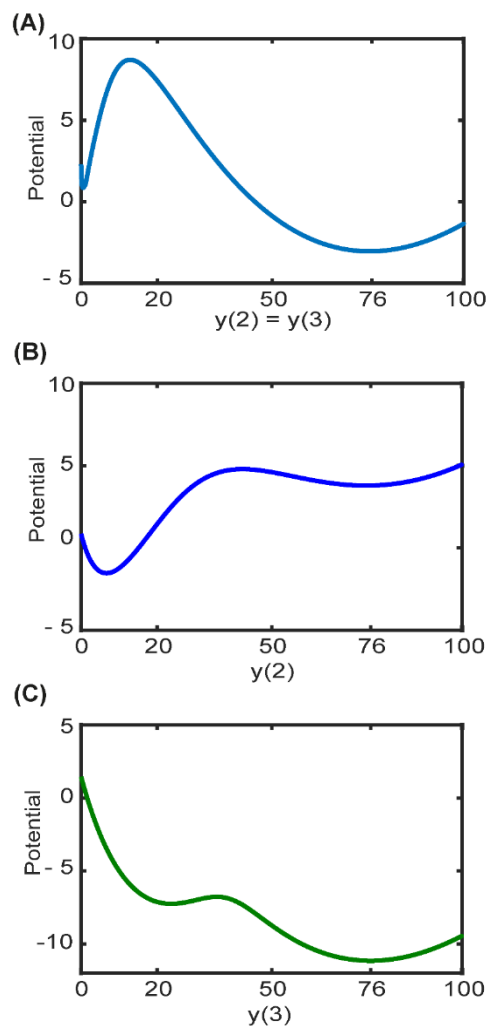


**Fig. F1** Stochastic potential profile of the MAN and MRN models

(A) Double-well potential of  $y(2) = y(3)$  in the MAN model. The parameters are given as  $S = 0$ ,  $K(1) = K(3) = 9$ ,  $K(2) = K(4) = 30$ ,  $k(3) = k(6) = 18.1$ ,  $k(4) = k(7) = 70.26$ ,  $k(5) = k(8) = 0.8$ ,  $b = 0.01$ ,  $n = 2$ .

(B, C) Double-well potential of  $y(2)$  (B) and of  $y(3)$  (C) in the MRN model. The parameters are given as  $S = 0$ ,  $K(1) = K(3) = 9$ ,  $K(2) = K(4) = 30$ ,  $k(3) = k(6) = 18.1$ ,  $k(4) = 85.30 >$   
 $k(7) = 43.1$ ,  $k(5) = k(8) = 0.8$ ,  $n = 4$ .

## References

- Acar M, Mettetal J, van Oudenaarden A (2008) Stochastic switching as a survival strategy in fluctuating environments. *Nat Genet* 40:471–475.
- Acar, M., Becskei, A., van Oudenaarden, A., 2005. Enhancement of cellular memory by reducing stochastic transitions. *Nature* 435, 228-232.
- Adam P. Arkin, 2001. Synthetic cell biology. *Current Opinion in Biotechnology*, 12(6):638–644.
- Ajo-Franklin, C. M., Drubin, D. A., Eskin, J. A., Gee, E. P., Landgraf, D., Phillips, I., Silver, P. A., 2007. Rational design of memory in eukaryotic cells. *Genes Dev* 21, 2271-2276.
- Alon, U., 2007. Network motifs: theory and experimental approaches. *Nat Rev Genet* 8, 450-461.
- Alves, R., Savageau, M. A., 2000. Extending the method of mathematically controlled comparison to include numerical comparisons. *Bioinformatics* 16, 786-798.
- Auslander, S., Auslander, D., Muller, M., Wieland, M., Fussenegger, M., 2012. Programmable single-cell mammalian biocomputers. *Nature* 487, 123-127.
- Ay, A., Arnosti, D. N., 2011. Mathematical modeling of gene expression: a guide for the perplexed biologist. *Crit Rev Biochem Mol Biol* 46, 137-51.
- Basu, S., Gerchman, Y., Collins, C. H., Arnold, F. H., Weiss, R., 2005. A synthetic multicellular system for programmed pattern formation. *Nature* 434, 1130-1134.
- Becskei, A., Seraphin, B., Serrano, L., 2001. Positive feedback in eukaryotic gene networks: cell differentiation by graded to binary response conversion. *EMBO J* 20, 2528-2535.
- Berg, O. G., 1978. A model for the statistical fluctuations of protein numbers in a microbial population. *J Theor Biol* 71, 587-603.

- Blake, W. J., M, K. A., Cantor, C. R., Collins, J. J., 2003. Noise in eukaryotic gene expression. *Nature* 422, 633-637.
- Brandman, O., Meyer, T., 2008. Feedback loops shape cellular signals in space and time. *Science* 322, 390-395.
- Burrill, D. R., Silver, P. A., 2010. Making cellular memories. *Cell* 140, 13-18.
- Cao, Y., Gillespie, D. T., Petzold, L. R., 2006. Efficient step size selection for the tau-leaping simulation method. *J Chem Phys* 124, 044109.
- Casadesus, J., D'Ari, R., 2002. Memory in bacteria and phage. *Bioessays* 24, 512-518.
- Cheng, Z., Liu, F., Zhang, X. P., Wang, W., 2008. Robustness analysis of cellular memory in an autoactivating positive feedback system. *FEBS Lett* 582, 3776-3782.
- Cherry, J. L., Adler, F. R., 2000. How to make a Biological Switch. *Journal of Theoretical Biology* 203, 117-133.
- Csete, M. E. and Doyle, J. C, 2002. Reverse engineering of biological complexity. *Science*, 295(5560):1664–1669.
- Daniel, R., Rubens, J. R., Sarpeshkar, R., Lu, T. K., 2013. Synthetic analog computation in living cells. *Nature* 497, 619-623.
- Doyle F.J. and Stelling J, 2006. Systems interface biology. *Journal of the Royal Society Interface*, 3(10):603–616.
- Drury, K. L. S., 2007. Shot noise perturbations and mean first passage times between stable states. *Theoretical Population Biology* 72, 153-166.
- Eldar, A., Elowitz, M. B., 2010. Functional roles for noise in genetic circuits. *Nature* 467, 167-173.
- Elowitz, M. B., Leibler, S., 2000. A synthetic oscillatory network of transcriptional regulators. *Nature* 403, 335-338.

- Elowitz, M. B., Levine, A. J., Siggia, E. D., Swain, P. S., 2002. Stochastic gene expression in a single cell. *Science* 297, 1183-1186.
- Ferrell JE, Jr., Machleder EM (1998) The biochemical basis of an all-or-none cell fate switch in *Xenopus* oocytes. *Science* 280: 895-898.
- Ferrell, J. E., Jr., 2002. Self-perpetuating states in signal transduction: positive feedback, double-negative feedback and bistability. *Curr Opin Cell Biol* 14, 140-148.
- Freeman, M., 2000. Feedback control of intercellular signalling in development. *Nature* 408, 313-319.
- Gardiner, C.W., 2009. *Stochastic Methods: A Handbook for the Natural and Social Sciences*. Springer Series in Synergetics, 4th ed. (Springer-Verlag, Berlin).
- Gardner, T. S., Cantor, C. R., Collins, J. J., 2000. Construction of a genetic toggle switch in *Escherichia coli*. *Nature* 403, 339-342.
- Gillespie, D. T., 1977. Exact Stochastic Simulation of Coupled Chemical-Reactions. *Journal of Physical Chemistry* 81, 2340-2361.
- Gillespie, D. T., 2000. The chemical Langevin equation. *Journal of Chemical Physics* 113, 297-306.
- Hasty et.al. 2001. Computational studies of gene regulatory networks: in numero molecular biology. *Nat Rev Genet.* 2001 Apr;2(4):268-79.
- Hasty, J., McMillen, D., Collins, J. J., 2002. Engineered gene circuits. *Nature* 420, 224-30.
- Hasty, J., Pradines, J., Dolnik, M., Collins, J. J., 2000. Noise-based switches and amplifiers for gene expression. *Proc Natl Acad Sci U S A* 97, 2075-2080.
- Huang, C. Y., Ferrell, J. E., Jr., 1996. Ultrasensitivity in the mitogen-activated protein kinase cascade. *Proc Natl Acad Sci U S A* 93, 10078-10083.
- Ideker, T. Galitski, and L. Hood., 2001. A new approach to decoding life: Systems biology. *Annual Review of Genomics and Human Genetics*, 2:343-372.

- Isaacs FJ, Hasty J, Cantor CR, Collins JJ (2003) Prediction and measurement of an autoregulatory genetic module. *Proc Natl Acad Sci U S A* 100: 7714-7719.
- José Mira and Camino González Fernández, 2003. Two Examples of Deterministic versus Stochastic Modeling of Chemical Reactions. *J. Chem. Educ.*, 2003, 80 (12), p 1488.
- Kaern, M., Blake, W. J., Collins, J. J., 2003. The engineering of gene regulatory networks. *Annu Rev Biomed Eng* 5, 179-206.
- Kim, S. Y., Ferrell, J. E., Jr., 2007. Substrate competition as a source of ultrasensitivity in the inactivation of Wee1. *Cell* 128, 1133-1145.
- Kitano, H 2002. Systems biology: A brief overview. *Science*, 295(5560):1662–1664.
- Kurata, H., El-Samad, H., Iwasaki, R., Ohtake, H., Doyle, J. C., Grigoroza, I., Gross, C. A., Khammash, M., 2006. Module-based analysis of robustness tradeoffs in the heat shock response system. *PLoS Comput Biol* 2, e59, doi:10.1371/journal.pcbi.0020059.
- Kurata, H., Inoue, K., Maeda, K., Masaki, K., Shimokawa, Y., Zhao, Q., 2007. Extended CADLIVE: a novel graphical notation for design of biochemical network maps and computational pathway analysis. *Nucleic Acids Res* 35, e134.
- Kurata, H., Maeda, K., Onaka, T., Takata, T., 2014. BioFNet: biological functional network database for analysis and synthesis of biological systems. *Brief Bioinform* 15, 699-709.
- Kurata, H., Matoba, N., Shimizu, N., 2003. CADLIVE for constructing a large-scale biochemical network based on a simulation-directed notation and its application to yeast cell cycle. *Nucleic Acids Res* 31, 4071-4084.
- Matsuda, M., Koga, M., Woltjen, K., Nishida, E., Ebisuya, M., 2015. Synthetic lateral inhibition governs cell-type bifurcation with robust ratios. *Nat Commun* 6, 6195, doi:10.1038/ncomms7195.
- McAdams, H. H., Arkin, A., 1997. Stochastic mechanisms in gene expression. *Proceedings of the National Academy of Sciences of the United States of America* 94, 814-819.

- Moon, T. S., Lou, C., Tamsir, A., Stanton, B. C., Voigt, C. A., 2012. Genetic programs constructed from layered logic gates in single cells. *Nature* 491, 249-253.
- Ochab-Marcinek A, Tabaka M (2010) Bimodal gene expression in noncooperative regulatory systems. *Proc Natl Acad Sci U S A* 107: 22096-22101.
- Ozbudak, E. M., Thattai, M., Kurtser, I., Grossman, A. D., van Oudenaarden, A., 2002. Regulation of noise in the expression of a single gene. *Nature Genetics* 31, 69-73.
- Palani S, Sarkar CA (2008) Positive receptor feedback during lineage commitment can generate ultrasensitivity to ligand and confer robustness to a bistable switch. *Biophysical Journal* 95: 1575-1589.
- Pawson, T., Linding, R., 2005. Synthetic modular systems--reverse engineering of signal transduction. *FEBS Lett* 579, 1808-14.
- Pedraza, J. M., van Oudenaarden, A., 2005. Noise propagation in gene networks. *Science* 307, 1965-1969.
- Peter S. Swain and Andre Longtin, 2006. Noise in genetic and neural systems. *Chaos*, 16:026101.
- Peter S. Swain, Michael B. Elowitz, and Eric D. Siggia, 2002. Intrinsic and extrinsic contributions to stochasticity in gene expression. *Proceedings of the National Academy of Sciences (U.S.A.)*, 99(20):12795–12800.
- Pomerening, J. R., Kim, S. Y., Ferrell, J. E., Jr., 2005. Systems-level dissection of the cell-cycle oscillator: bypassing positive feedback produces damped oscillations. *Cell* 122, 565-578.
- Raser, J. M., O'Shea, E. K., 2004. Control of stochasticity in eukaryotic gene expression. *Science* 304, 1811-4.
- Risken, H., and Frank, T., 1996. *The Fokker–Planck Equation: Methods of Solution and Applications*, 2nd ed. (Springer, Berlin).

- Scott, M., Hwa, T., Ingalls, B., 2007. Deterministic characterization of stochastic genetic circuits. *Proceedings of the National Academy of Sciences of the United States of America* 104, 7402-7407.
- Sharma, Y., Dutta, P. S., Gupta, A. K., 2016. Anticipating regime shifts in gene expression: The case of an autoactivating positive feedback loop. *Phys Rev E* 93, 032404.
- Shopera, T., Henson, W. R., Ng, A., Lee, Y. J., Ng, K., Moon, T. S., 2015. Robust, tunable genetic memory from protein sequestration combined with positive feedback. *Nucleic Acids Res* 43, 9086-94.
- Shu CC, Chatterjee A, Dunny G, Hu WS, Ramkrishna D (2011) Bistability versus bimodal distributions in gene regulatory processes from population balance. *PLoS Comput Biol* 7: e1002140.
- Tabor, J. J., Salis, H. M., Simpson, Z. B., Chevalier, A. A., Levskaya, A., Marcotte, E. M., Voigt, C. A., Ellington, A. D., 2009. A synthetic genetic edge detection program. *Cell* 137, 1272-1281.
- Tan, C., Marguet, P., You, L., 2009. Emergent bistability by a growth-modulating positive feedback circuit. *Nat Chem Biol* 5, 842-848.
- Thattai, M., van Oudenaarden, A., 2001. Intrinsic noise in gene regulatory networks. *Proc Natl Acad Sci U S A* 98, 8614-9.
- Thomas, P., Straube, A. V., Grima, R., 2011. Communication: limitations of the stochastic quasi-steady-state approximation in open biochemical reaction networks. *J Chem Phys* 135, 181103.
- Thomas, P., Popovic, N., Grima, R., 2014. Phenotypic switching in gene regulatory networks. *Proceedings of the National Academy of Sciences of the United States of America* 111, 6994-6999.
- Tian T, Burrage K (2006) Stochastic models for regulatory networks of the genetic toggle switch. *Proc Natl Acad Sci U S A* 103: 8372-8377.

- Tyo, K. E., Alper, H. S., Stephanopoulos, G. N., 2007. Expanding the metabolic engineering toolbox: more options to engineer cells. *Trends Biotechnol* 25, 132-7.
- Wang, B., Kitney, R. I., Joly, N., Buck, M., 2011. Engineering modular and orthogonal genetic logic gates for robust digital-like synthetic biology. *Nat Commun* 2, 508.
- Wang, L., Qian, K., Huang, Y., Jin, N., Lai, H., Zhang, T., Li, C., Zhang, C., Bi, X., Wu, D., Wang, C., Wu, H., Tan, P., Lu, J., Chen, L., Li, K., Li, X., Wang, D., 2015. SynBioLGDB: a resource for experimentally validated logic gates in synthetic biology. *Sci Rep* 5, 8090.
- Wilhelm T (2009) The smallest chemical reaction system with bistability. *BMC Syst Biol* 3: 90.
- Xiong, W., Ferrell, J. E., 2003. A positive-feedback-based bistable 'memory module' that governs a cell fate decision. *Nature* 426, 460-465.
- Zhang, H., Chen, Y., Chen, Y., 2012. Noise propagation in gene regulation networks involving interlinked positive and negative feedback loops. *PLoS One* 7, e51840.

## **Acknowledgements**

Firstly, I would like to thank my supervisor, Professor **Dr. Hiroyuki Kurata**, for having introduced me to bioinformatics, for all the knowledge he has transmitted me, and for the motivation he has always help in my work. Thank you for the patience and energy you granted me during all this time, and in spite of the difficult start which I had. I would also like to thank the Kurata Laboratory, Department of Bioscience and Bioinformatics, Faculty of Computer Science and System Engineering, Kyushu Institute of Technology, and in particular Kurata Sensei for having financed me and permitted me this grand opportunity to initiate myself with this research.

Special thanks to the co-supervisors Professor Dr. Tetsushi Yada, Professor Dr. Shunsuke Aoki, for the insightful comments, suggestions, and encouragement during the presentations. Above all, we are grateful to Dr. Kazuhiro Maeda for his helpful technical support to improve the spread of the stochastic simulation and useful discussions. Furthermore, I wish to thank Dr. Yu Matsuoka and all Kurata Lab members for having supported.

Finally, I dedicate this paragraph to my mother, my father and my sister, to whom I owe everything, and without whom I would probably never have reached where I am now. Thank you for leaving me freedom of expression, for so many dialogues exchanged, and for listening to me and bestowing me with your confidence and trust. Thank you for being by my side!

**A.B.M. Shamim Ul Hasan**

Graduate School of Computer Science and System Engineering

Kyushu Institute of Technology (KIT)